AFRL-RX-TY-TR-2012-0038

FIRE PROTECTION SAFETY EVALUATIONS OF HYDRO-TREATED RENEWABLE JET (HRJ) AND SYNTHETIC PARAFFINIC KEROSENE (SPK) FUELS

Steven P. Wells and Mark A. Enlow
Applied Research Associates
421 Oak Avenue
Panama City, FL 32401

Howard Mayfield
Airbase Technologies Division
Air Force Research Laboratory
139 Barnes Drive, Suite 2
Tyndall Air Force Base, FL 32403-5323

April 2012

AIR FORCE RESEARCH LABORATORY
MATERIALS AND MANUFACTURING DIRECTORATE

■ **Air Force Materiel Command** ■ **United States Air Force** ■ **Tyndall Air Force Base, FL 32403-5323**

DISCLAIMER

Reference herein to any specific commercial product, process, or service by trade name, trademark, manufacturer, or otherwise does not constitute or imply its endorsement, recommendation, or approval by the United States Air Force. The views and opinions of authors expressed herein do not necessarily state or reflect those of the United States Air Force.

This report was prepared as an account of work sponsored by the United States Air Force. Neither the United States Air Force, nor any of its employees, makes any warranty, expressed or implied, or assumes any legal liability or responsibility for the accuracy, completeness, or usefulness of any information, apparatus, product, or process disclosed, or represents that its use would not infringe privately owned rights.

NOTICE AND SIGNATURE PAGE

Using Government drawings, specifications, or other data included in this document for any purpose other than Government procurement does not in any way obligate the U.S. Government. The fact that the Government formulated or supplied the drawings, specifications, or other data does not license the holder or any other person or corporation; or convey any rights or permission to manufacture, use, or sell any patented invention that may relate to them.

This report was cleared for public release by the 88th Air Base Wing Public Affairs Office at Wright Patterson Air Force Base, Ohio available to the general public, including foreign nationals. Copies may be obtained from the Defense Technical Information Center (DTIC) (http://www.dtic.mil).

AFRL-RX-TY-TR-2012-0038 HAS BEEN REVIEWED AND IS APPROVED FOR PUBLICATION IN ACCORDANCE WITH ASSIGNED DISTRIBUTION STATEMENT.

WALTZ.WALTER.M.1006453097 Digitally signed by WALTZ.WALTER.M.1006453097 DN: c=US, o=U.S. Government, ou=DoD, ou=PKI, ou=USAF, cn=WALTZ.WALTER.M.1006453097 Date: 2012.06.11 10:37:58 -05'00'

WALTER M. WALTZ, DR-III
Work Unit Manager

WALTZ.WALTER.M.1006453097 Digitally signed by WALTZ.WALTER.M.1006453097 DN: c=US, o=U.S. Government, ou=DoD, ou=PKI, ou=USAF, cn=WALTZ.WALTER.M.1006453097 Date: 2012.06.11 10:26:04 -05'00'

WALTER M. WALTZ, DR-III
Program Manager

RHODES.ALBERT.N.III.1175488622 Digitally signed by RHODES.ALBERT.N.III.1175488622 DN: c=US, o=U.S. Government, ou=DoD, ou=PKI, ou=USAF, cn=RHODES.ALBERT.N.III.1175488622 Date: 2012.06.25 10:25:21 -05'00'

ALBERT N. RHODES, PhD
Chief, Airbase Technologies Division

This report is published in the interest of scientific and technical information exchange, and its publication does not constitute the Government's approval or disapproval of its ideas or findings.

REPORT DOCUMENTATION PAGE

Form Approved
OMB No. 0704-0188

PLEASE DO NOT RETURN YOUR FORM TO THE ABOVE ADDRESS.

1. REPORT DATE *(DD-MM-YYYY)*	2. REPORT TYPE	3. DATES COVERED *(From - To)*
30-APR-2012	Interim Technical Report	01-MAY-2010 -- 30-SEP-2011

4. TITLE AND SUBTITLE

Fire Protection Safety Evaluations of Hydro-Treated Renewable Jet (HRJ) and Synthetic Paraffinic Kerosene (SPK) Fuels

5a. CONTRACT NUMBER

FA4819-09-C-0030

5b. GRANT NUMBER

5c. PROGRAM ELEMENT NUMBER

0909999F

6. AUTHOR(S)

*Wells, Steven P.; *Enlow, Mark A.; ^Mayfield, Howard T.

5d. PROJECT NUMBER

GOVT

5e. TASK NUMBER

D0

5f. WORK UNIT NUMBER

QD103001

7. PERFORMING ORGANIZATION NAME(S) AND ADDRESS(ES)

Applied Research Associates
421 Oak Drive
Panama City, FL 32401

8. PERFORMING ORGANIZATION REPORT NUMBER

9. SPONSORING/MONITORING AGENCY NAME(S) AND ADDRESS(ES)

Air Force Research Laboratory
Materials and Manufacturing Directorate
Airbase Technologies Division
139 Barnes Drive, Suite 2
Tyndall Air Force Base, FL 32403-5323

10. SPONSOR/MONITOR'S ACRONYM(S)

AFRL/RXQES

11. SPONSOR/MONITOR'S REPORT NUMBER(S)

AFRL-RX-TY-TR-2012-0038

12. DISTRIBUTION/AVAILABILITY STATEMENT

Distribution A: Approved for public release; distribution unlimited.

13. SUPPLEMENTARY NOTES

Ref Public Affairs Case # 88ABW-2012-3666, 27 June 2012. Document contains color images.

14. ABSTRACT

Alternative liquid jet fuels are being considered as a replacement for petroleum-based fuels for use in United States Air Force (USAF) aircraft and support equipment and vehicles. As with any new weapons system or other type of potential fire threat, the fire protection safety risk to the first responder must be established. The objective of this study was to measure alternative fuel safety parameters. Flame propagation tests documented the flame spread rate on liquid fuel surfaces. Flame visible spectrum emissions were measured in normal and elevated oxygen concentration environments. Commercial optical flame detectors (OFDs) and commercial combustible gas detectors (CGDs) were evaluated for their relative response to and ability to detect bio-oil derived hydroprocessed renewable jet (HRJ) and synthetic paraffinic kerosene (SPK) fuel fires and vapors as compared to JP-8.

15. SUBJECT TERMS

hydroprocessed renewable jet fuel, HRJ, flame propagation, optical flame detector, combustible gas detector, alternative fuel, JP-8, Synthetic Paraffinic Kerosene (SPK)

16. SECURITY CLASSIFICATION OF:			17. LIMITATION OF ABSTRACT	18. NUMBER OF PAGES	19a. NAME OF RESPONSIBLE PERSON
a. REPORT	b. ABSTRACT	c. THIS PAGE			Walter M. Waltz
U	U	U	UU	63	19b. TELEPHONE NUMBER *(Include area code)*

Reset

Standard Form 298 (Rev. 8/98)
Prescribed by ANSI Std. Z39.18

TABLE OF CONTENTS

LIST OF FIGURES

Page

LIST OF TABLES

ACKNOWLEDGEMENTS

The authors would like to recognize the contributions of Detector Electronics Corporation (Det-Tronics), MSA, and RAE Systems to this study.

1. SUMMARY

Alternative liquid jet fuels are being considered as a replacement for petroleum-based fuels by the United States Air Force (USAF). Bio-oil derived hydroprocessed renewable jet (HRJ) fuels, also known as hydroprocessed esters and fatty acids (HEFA) fuels, are alternative fuels that are blended 50/50 with conventional Jet Propellent-8 (JP-8) and are being evaluated for use in USAF aircraft and support equipment and vehicles (SE&V). As with any new weapons system or other type of potential fire threat, the fire protection safety risk to the first responder must be established. Safety parameters that are critical with liquid jet fuels include flame speed propagation, flame visible spectrum emissions, the ability of aircraft hangar automatic flame detectors to recognize and provide an alarm to a fuel fire, and ability of vapor detectors to recognize the potential for the presence of explosive concentrations of fuel vapors. Testing was performed at the request of the Aeronautical Systems Center Alternative Fuels Certification Division (ASC/WNN).

The objective of this study was to measure alternative fuels for the safety properties of flame speed propagation, flame visible spectrum emissions, and compatibility with vapor and flame detectors. The results will provide data for fire protection safety and provide the USAF firefighter with the knowledge required for rapid decision making and the best incident response in the event of an accidental fuel spill or fire. Flame propagation tests documented the flame spread rate on liquid fuel surfaces from room temperature, below the fuel flash point, up to fuel temperatures above the fuel flash points. Flame visible spectrum emissions were measured in normal and elevated oxygen concentration environments. Commercial optical flame detectors (OFDs) were evaluated for their ability to detect HRJ and synthetic paraffinic kerosene (SPK) fuel fires as compared to their ability to detect JP-8 fires. Commercial combustible gas detectors (CGDs) were evaluated to determine whether alternative fuel vapors can be detected by typical CGDs that are utilized by the USAF and to determine the relative response of each fuel to JP-8.

Significant safety issues with these alternative fuels, as compared to JP-8 fuel, did not emerge in these evaluations. Notable safety observations were that the temperature at which the flame propagation rate changes from low speed to high speed varied marginally in the fuels with flash point, no flame visibility issues were observed, and optical flame and combustible gas detectors will respond to these fuels or fires involving them.

2. INTRODUCTION

2.1. Background

Alternative liquid jet fuels are being considered as a replacement for petroleum-based fuels by the USAF. Bio-oil derived HRJ fuels, also known as HEFA fuels, are alternative fuels that are being evaluated for use in USAF aircraft and SE&V. Some SPK alternative fuels have previously been certified for use in USAF aircraft and SE&V. In these evaluations, the alternative fuel is blended 50/50 with conventional JP 8.

As with any new weapons system or other type of potential fire threat, the fire protection safety risk to the first responder must be established. Safety parameters that are critical with liquid jet fuels include flame speed propagation, flame visible spectrum emissions, the ability of aircraft hangar automatic flame detectors to recognize and provide an alarm to a fuel fire, and ability of vapor detectors to recognize the potential for the presence of explosive concentrations of fuel vapors. Testing was performed at the request of ASC/WNN.

Fire safety detection standards are promulgated by the American National Standards Institute (ANSI) and by Factory Mutual (FM). Applicable standards from these organizations have been utilized in this study.

2.1.1. Flame Speed Propagation

Flame speed propagation defines the speed at which a flame front will propagate across the surface of a fuel spill. This property impacts how fast fires will grow to full intensity and the required speed of response for fire departments and/or suppression systems. Propagation of a flame front below a fuel's flash point is typically maintained by flame radiation heating the fuel in front of the advancing flame to its flash point creating flammable vapors that ignite. For fuels at temperatures exceeding their flash point, flame speed is greater since flammable vapors are already present and don't have to be created by flame radiation. Flame speed is by and large affected by fuel temperature and flashpoint. The flame speed contributes to the hazard associated with each fuel and determines how fast a fuel spill fire can become difficult to control with available fire protection resources.

2.1.2. Flame Visible Spectrum Emissions

Flame emissions in the visible spectrum are an important safety parameter for fuel fires. The lack of visible emissions from fuel flames increases the difficulty of fighting fire and the risk for first responders. Knowledge of whether a fuel flame will be visible greatly affects how operations are conducted in the vicinity of the use of that fuel. A previous study by Lille [1] has documented the decrease in flame visibility from reduced oxygen levels. USAF operations include accident scenarios where fuel fires can occur from common fuel spills, from airplane crashes, and from incidents that involve large quantities of fuel and chemicals that allow the fuel to burn in an oxygen rich environment. This latter scenario raises the question of how an oxygen rich environment affects visible spectrum emissions in existing and emerging fuels.

2.1.3. Optical Flame Detection

Hangar optical flame detector sensors monitor for flame emissions in the ultraviolet (UV), visible, and infrared (IR) regions of the electromagnetic spectrum. Typically these measurements

include regions of the electromagnetic spectrum from 0.8 nm (ultraviolet) to 8 μm (infrared). Using data from its sensors, the detector logic verifies that a fuel fire exists and signals an alarm that can notify building occupants, notify the fire department, or activate an installed fire suppression system.

Unfortunately, there are many non-fire sources of the same 0.8 nm to 8 μm spectral radiation from hangar operations that can confuse the detector optics and programming and subsequently cause false alarms that can be costly to the USAF due to fire department response, maintenance, and false activations of suppressant systems. As a result, the flame detectors must also be programmed to discriminate against this non-fire radiation. The commercially available OFDs that provide the greatest detection distances and superior false alarm immunity are multispectral IR devices (typically three IR sensors) as reported in NRL/MR/6180-00-8457 [2]. There are several manufacturers that have detectors of this type available and some of these detectors have previously been listed by Factory Mutual (FM) for jet fuel fires. Existing OFDs have not previously been evaluated for response to fires involving alternative HRJ or SPK fuels.

In addition to spectral radiation, electromagnetic interference from aircraft avionics can bypass the detector optics and cause alarms from induced voltage/current in the detection system electronics. This threat must be considered when acquiring an aircraft hangar optical detection system. A new detection system option combats this avionics threat by replacing traditional communication (relay closures or 4-20 mA signals) between the detector and the facility control panel with a digital communication system that is more immune to this interference. The downside to the digital communications is a slight increase in flame detection alarm time. This system was not evaluated in this study.

For an optical flame detector to receive FM approval, the detector must perform as outlined in ANSI/FM 3260[3]. One of the required tests is flame response sensitivity that requires a detector to alarm in 30 s or less. Average measured detection times for each fuel, pan size, and distance are recorded and are used when detectors are marketed and specified. Therefore, a specific detector manufacturer may report FM test results of an average response time that is less than 30 s for a particular fuel at a particular distance and pan size (i.e. n-Heptane, 210 ft, 1- × 1-ft pan fire, 15-s average detection response).

Flame detection performance of OFDs is traditionally evaluated against 1- × 1-ft and 2- × 2-ft fuel fires. USAF Engineering Technical Letter (ETL) 02-15, section A1.3.5.3 discusses guidance for the type and performance of OFDs that can be used in USAF aircraft hangars. The types of detectors include multi-spectrum detectors that include IR or UV sensors. It also states that a detector should “detect a fully developed 10- × 10-ft JP-4, JP-8, or JET-A fuel fire at a minimum distance of 148 ft, within 5 s”.[4]

When comparing a detector’s performance against new fuels, any of these size and distance tests will provide the data necessary to determine if the fuel fire can be reliably detected.

Existing OFDs have not previously been evaluated for response to fires involving these new fuels. Figure 1 shows photographs of fully involved 6-ft diameter fuel fires with each of these fuels. From these images it can be seen that in the visible portion of the electromagnetic

spectrum that differences in fires involving JP-8 and these fuels do exist including varying degrees of soot production. Differences in infrared emissions, and the resulting effect on optical flame detector response, require additional investigation.

Figure 1. Photographs of Fully Involved 6-ft Diameter Fuel Fires

2.1.4. Combustible Gas Detectors (CGDs)

Handheld vapor detectors are used for numerous operations in the USAF to monitor atmospheres for oxygen, other toxic gases, and combustible concentrations of flammable liquid fuel vapors to ensure that environments are not immediately dangerous to life and health. These operations include confined space entry, such as fuel tank inspection and repair, and USAF emergency management (EM) operations.

CGDs measure the percentage of gas in an atmosphere as related to the lower explosive limit (LEL) of that gas. Technical Order (TO) 1-1-3 defines fire safe as "an atmospheric concentration of combustible vapors equal to or less than 20% LEL or (1200 ppm)" and entry safe as "10% LEL or (600 ppm)".[5] CGDs can be used to monitor threshold limit values (TLVs) or permissible exposure limits. TLV is the concentration of a substance that a person can be exposed to without adverse health effects and is measured in time weighted average, short term exposure limit, or ceiling.

The typical technologies employed in CGDs for detecting volatile organic compounds (VOCs) and combustible gases are photoionization detectors (PID), catalytic bead, and infrared. These detectors typically provide a digital display that reports concentrations of detected gases. Most also have visible and/or audible alarms when a dangerous environment is detected. PIDs are often preferred due to their low-level detection, response time, cost, and maintenance.

The CGDs are calibrated for specific gases, and correction factors, or response factors, are used for numerous additional fuels. For example, when using a CGD in areas where JP-8 jet fuel is expected, the detector is calibrated for a similar gas such as isobutylene, and a correction/response factor for JP-8 is used for an accurate indication by the instrument. Some instruments have the correction/response factors built in.

For open fuel tank/cell repair, TO 1-1-3 authorizes a photo ionization detector (PID), NSN 6665-01-457-0472.[5] Air Force Manual AFMAN 10-2057 states that the USAF will maintain EM response capabilities including a multi gas monitor.[6]

Among the detectors used by the USAF are the MultiRAE Plus manufactured by RAE Systems Inc. shown in Figure 2, and the Passport® PID II Organic Vapor Monitor manufactured by Mine Safety Appliances (MSA). RAE Systems has a replacement unit for the MultiRAE Plus, released in 2011, called the MultiRAE Family. MSA has discontinued selling the Passport® PID II and has two potential replacements: the Sirius™ Multi-Gas Detector, shown in Figure 2, and the ALTAIR® 5 Multigas Detector. The USAF also has additional gas detectors in their inventory that vary by manufacturer and model. The RAE Systems Inc. MultiRAE (MultiRAE Plus) and the MSA Sirius™ detectors were evaluated herein with JP-8 and alternative fuels.

Figure 2. RAE Systems MultiRAE (left) and MSA Sirius™ (right)
Photos from: http://www.raesystems.com/products/multirae-plus and http://www.msanorthamerica.com/catalog/product684.html.

2.2. Objective

The objective of this study was to evaluate alternative fuels for the safety properties of flame speed propagation, flame visible spectrum emissions, and compatibility with vapor and flame detectors. The results will provide data for fire protection safety and provide the USAF firefighter with the knowledge required for rapid decision making and the best incident response in the event of an accidental fuel spill or fire.

2.3. Scope

Flame propagation tests documented the flame spread rate on liquid fuel surfaces from room temperature below the fuel flash point up to fuel temperatures above the fuel flash points. Flame visible spectrum emissions were measured in normal and elevated oxygen concentration environments. Commercial OFDs were evaluated for their ability to detect HRJ and SPK fuel fires as compared to their ability to detect JP-8 fires. Commercial CGDs were evaluated to determine whether alternative fuel vapors can be detected by typical CGDs that are utilized by the USAF and to determine the relative response of each fuel compared to the response to JP-8.

3. METHODS, ASSUMPTIONS, AND PROCEDURES

Two HRJ fuels and one Fischer-Tropsch (F-T) SPK fuel were evaluated. The two HRJ fuels were Camelina bio-oil derived SPK and Tallow bio-oil derived SPK both manufactured by UOP LLC. The F-T fuel was Shell's F-T iso-paraffinic kerosene. Conventional JP-8 jet fuel (MIL-DTL-83133F) was also evaluated as a baseline.

Since alternative fuels are blended 50/50 with JP-8 for use in USAF aircraft, the threat from alternative fuels also includes these blends. In addition to the four fuels mentioned above, three alternative fuel/JP-8 50/50 blends were also evaluated for a total of seven fuels and fuel blends.

3.1. Flame Speed Propagation

Flame speed propagation tests measured the rate at which the flame front moved across a liquid fuel spill on water. No standard test protocols are available for these liquid fuel spill flame propagation evaluations, so a protocol was established based on previous similar measurements including work reported on in AFRL-ML-TY-TR-1998-4504.[7] Flame propagation rates for the seven fuels and fuel mixtures at temperatures ranging from room temperature to approximately 190 °F were measured.

Flame spread tests were conducted using a custom built apparatus consisting of a triangular-bottomed steel trough that was 48 inches long, 3.9 inches wide at the top, and 1.2 inches in depth. Omegalux silicon-rubber flexible heater strips were applied to the underside of the trough so that the trough could be pre-heated for experiments involving elevated temperatures. A type J thermocouple was embedded between the heater strips and the trough, which was then connected along with the heater strips to a Cole-Parmer Digi-sense temperature controller. Note that for elevated temperature measurements, both the flame spread trough and the fuel sample were pre-heated to the desired temperature before testing.

Evaluations were performed inside a 5- × 8-ft walk-in laboratory hood. During the experiment the exhaust system was turned off to ensure still air in the hood. All experiments were videotaped using a digital video camera capturing footage at 30 frames/s. To perform the experiment, a human operator, wearing lab coat and a full face shield, set the experiment up, then started the data collection and ignited the fuel with a torch. The operator exited the hood and remained outside until the flame propagation was complete and then re-engaged the exhaust system before re-entering the hood to smother the remaining fuel.

The trough was filled by first adding 0.21 gal of water. This was sufficient to fill the trough to approximately half its depth and was intended to reduce the amount of fuel needed during testing and to aid in pre-heating the trough by adding to the thermal capacity of the trough during elevated temperature experiments. During elevated temperature tests, the temperature controller was set and the trough was allowed to reach the desired temperature. The fuel sample was then added. Approximately 0.42 gal of fuel was added to bring the level to the top of the trough in an attempt to eliminate any edge effects due to the metal sides of the trough.

Fuel samples were prepared using a 2-L Erlenmeyer flask containing a stirring magnet and placed on a stirring hot plate. Fuels and fuel mixtures were stirred for a minimum of 15 min prior

to testing. Fuels to be tested at elevated temperatures were then heated to the desired temperature, using a type K thermocouple attached to a digital multi-meter to monitor the temperature. A watch glass was placed over the top of the flask to minimize evaporation loss during mixing and heating. Figure 3 shows a fuel sample being prepared.

Figure 3. Fuel Sample being Mixed and Heated in Preperation for a Test

The fuel was ignited at one end of the trough using a propane torch and allowed to propagate and become fully involved. Figure 4 shows a test where the flame has propagated across approximately two-thirds of the distance along the test apparatus.

Figure 4. Flame Speed Propagation Test in Progress

The advancement of the flame front was detected using thermocouples installed 0.25 in above the fuel surface. A total of five thermocouples were installed, the first placed 10 in from the ignition point in the trough and the remaining four placed at further intervals of 8 in along the trough. One additional thermocouple was positioned in the trough 0.5 in below the level of the fuel in order to monitor the fuel temperature. The thermocouples were beaded 24 gauge, K-type with a 1.3-s response time. Data from the thermocouples was measured at 50 Hz. The flame

spread rates were calculated using the time at which the temperature exceeded a temperature of 100 °F at each thermocouple.

It was hoped that the thermocouple data would show an abrupt increase in temperature corresponding to the point in time at which the flame front reached each thermocouple. However, initial experiments showed a gradual and irregular temperature increase. It was suspected that radiant heat from the advancing flame front was heating the thermocouples before the flame front reached the thermocouple itself. Figure 5 presents the thermocouple measurements from a flame spread experiment using JP-8 that displays this effect.

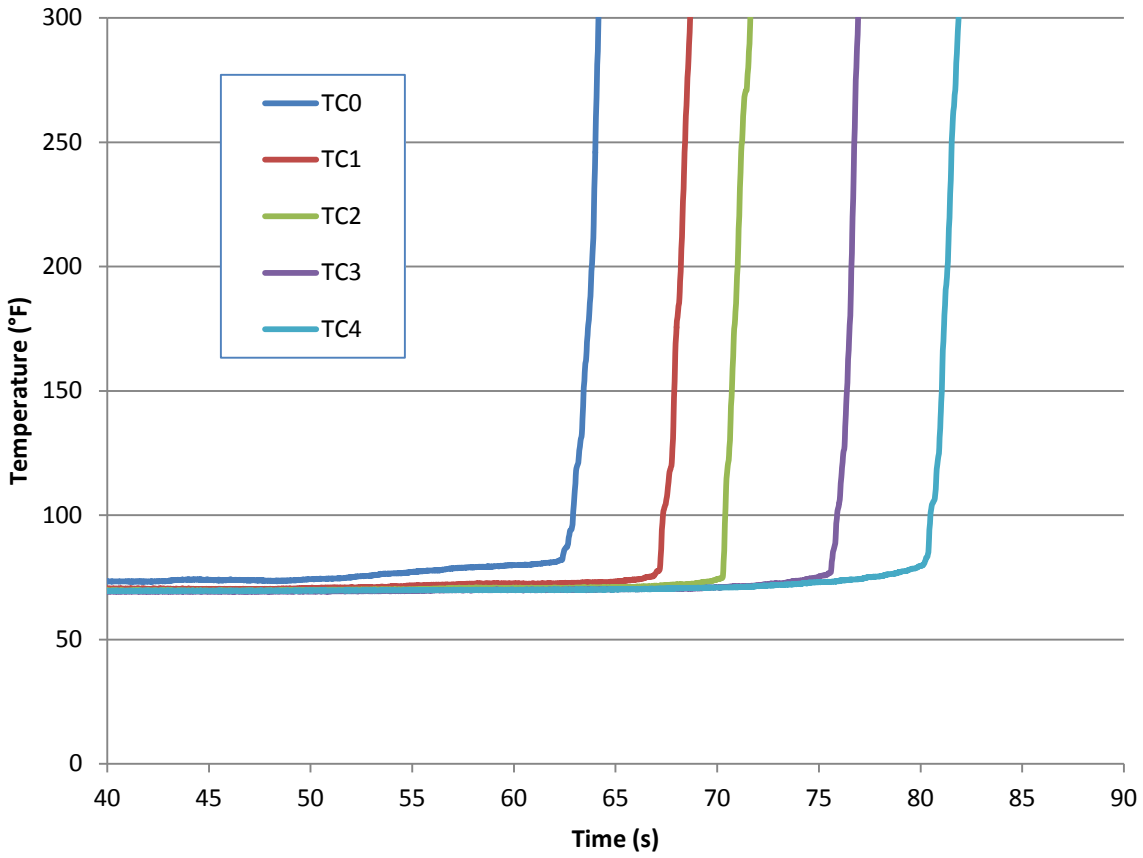

Figure 5. Thermocouple Data from a JP-8 Flame Spread Test with No Radiation Shields

To remedy this, simple radiation shields were constructed by folding 0.5- × 1-in rectangles of aluminum foil around the tip of each thermocouple so that they shielded the thermocouple from the advancing flame front. These shields were consumed during testing and had to be replaced after each test. See Figure 6 for a diagram and photo of this construct.

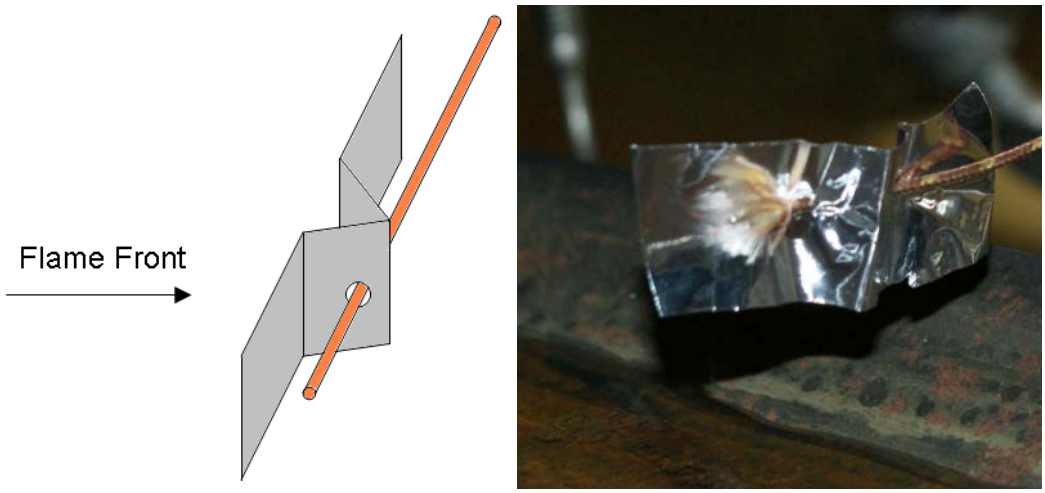

Figure 6. Schematic (left) and Photo (right) of the Aluminum Foil Radiation Shield used to Protect Each Thermocouple

Tests incorporating this radiation shield resulted in more defined onset temperatures. Figure 7 shows a flame spread experiment on JP-8 using the radiation shields to isolate the thermocouples.

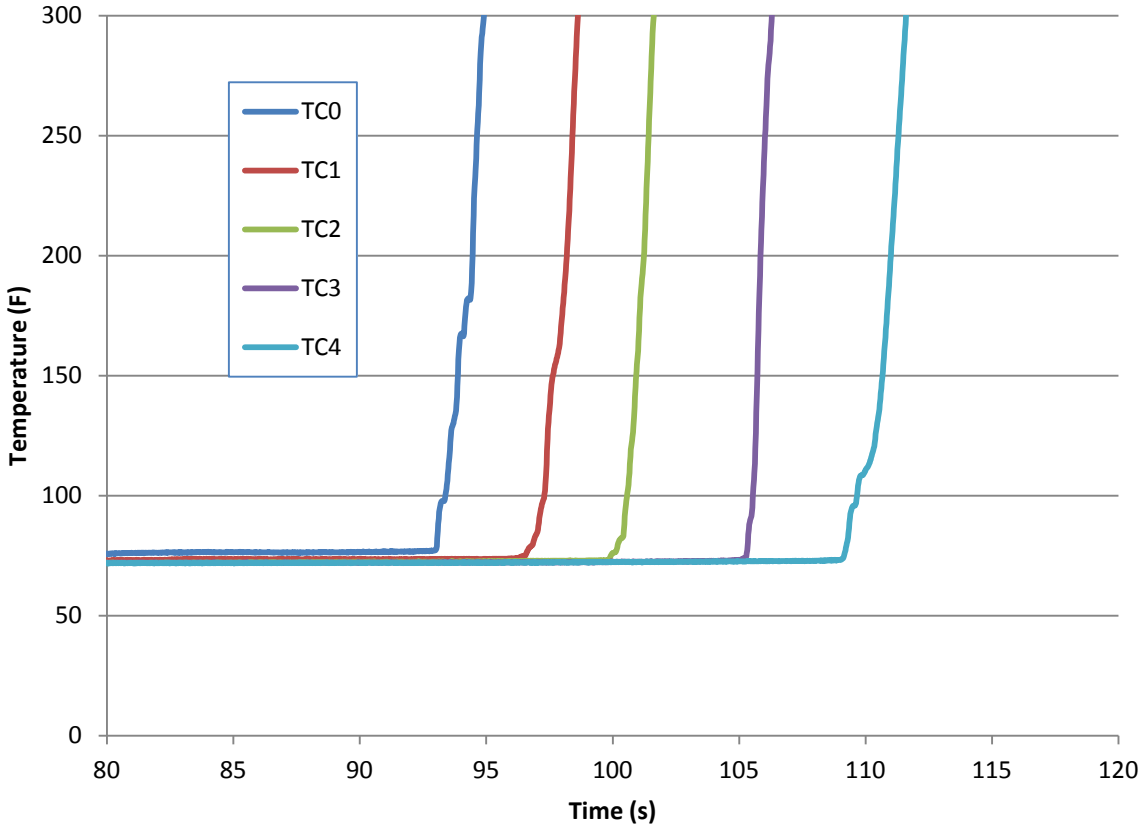

Figure 7. Thermocouple Data from a JP-8 Flame Spread Test Utilizing Radiation Shields

The thermocouple data proved sufficient for flame propagation rate determinations at low temperatures where the propagation rates were on the order of 5 to 10 in/s. However, at elevated fuel temperatures the flame front reached speeds of up to 70 in/s. At those rates the thermocouple data was no longer sufficient due to the relatively slow thermocouple response time. In those cases, a video recording was used to estimate flame propagation rates by determining the number of frames it took for the flame front to progress across known points in the apparatus. In general, thermocouple data was used to calculate flame propagation rates at temperatures below the fuel's flash points, while video footage was used to calculate flame propagation rates at temperatures above the fuel's flash points.

3.1.1. Soot Production Analysis

A measurement of soot production was carried out during selected tests by stationing clean substrate materials in the walk-in hood near the flame speed apparatus while test fires were conducted. Soot particles settled on these horizontal surfaces during the course of the fire experiment. The collected soot particles were sampled with 1- × 1-in squares of white sticky-pad media, cut from larger sheets (American CleanStat, Tackymat, product no. 183602WW-460). Initial experiments were conducted with horizontal collection substrates of aluminum foil, white 8.5- × 11-in sheets of copier & printer paper, and directly exposed 1- × 1-in single sheets from white sticky pads positioned with the sticky side up. Initial tests revealed that the white sticky pads were the most efficient collection substrate. Later tests were performed using only the white sticky pads. The substrates were positioned in the walk-in hood prior to the start of a flame propagation test and they remained throughout the fire and approximately 5 min of settling time before they were removed and sampled.

Sampling from the exposed substrates was conducted on an adjacent laboratory bench. Fresh 1-× 1-in sections of sticky pad were pressed to the aluminum foil or paper substrates to capture smoke particles and then removed and pressed to the bottom of a clean microscope slide. The top sheet of the sticky pad, now stuck to the microscope slide, was detached from the sticky pad to expose a clean sheet which was used to collect the next sample. Directly exposed sticky sheets were simply pressed on the bottom of a clean microscope slide. Each slide was labeled as soon as it was prepared by writing with a glassware marker on the frosted label area at one end of the slide. The slides were stored in a covered container until they could be examined with a microscope.

Microscopic examinations were made with a tri-ocular microscope ((Southern Precision Instruments, SPI 1864) equipped with dual 10X eyepieces and an auxiliary optical tube for camera mounting. A digital microscope camera (Motic, Moticam 2500) with resolution up to 5 megapixels was used to obtain photographs of the prepared slides. The Moticam 2500 was attached to the microscope's auxiliary optical tube through an optical adapter with a nominal 10X magnification, matching the eyepieces. Although the nominal magnifications of the eyepiece-objective combinations matched the camera-adapter-objective combination, the overall field of view of the camera was less than that of the eye and the effective magnifications of the photomicrographs were higher than the images viewed by the observer's eye. The images from the microscope camera were acquired, stored, and organized through Motic Images 2.0 software running on a Dell 610 laptop computer, which interfaced with the camera via a USB 2.0 interface. The microscope images were stored in a Joint Photographic Experts Group (JPEG or

.jpg) format at 1280 × 1024 pixel resolution (1.3 megapixels). For each mounted slide of sticky pad and particulates, attempts were made to image nine fields of view, one at each corner, one in the center of each side of the square pad, and one in the center. The planned nine observations were not always possible where edge damage distorted one of the planned areas.

The JPEG images were analyzed to locate, count, and quantify the smoke particles visible from each field of view. The MATLAB system (MATLAB, version 7.11, release R2010a, Mathworks, Inc.) equipped with the Image Processing Toolbox, version 7.1 was used to analyze the images. The image interpretation algorithm has been described previously and the procedures were used without change.[8] A MATLAB script (m-file) was used to convert the original color image to a binary black-and-white equivalent image using a threshold grayscale value selected by the analyst through an iterative process, and then to count the total number of particles, represented as black spots on the image, and their total pixel area. The count of particles and their total area were reported to the analyst.

3.2. Flame Visible Spectrum Emissions

A cup burner apparatus manufactured by Kidde-Fenwal was used to burn fuel samples under controlled atmospheric conditions for these tests. The cup burner consists of an inner quartz cylinder of approximately 0.5-in diameter, the “cup”, which is connected to either a liquid or a gaseous fuel supply. This inner cylinder is surrounded by an outer quartz cylinder approximately four inches in diameter. A controlled atmosphere of any desired composition may be directed through the outer cylinder in order to study the behavior of a burning fuel in that particular environment. Figure 8 displays the structure of the cup burner apparatus.

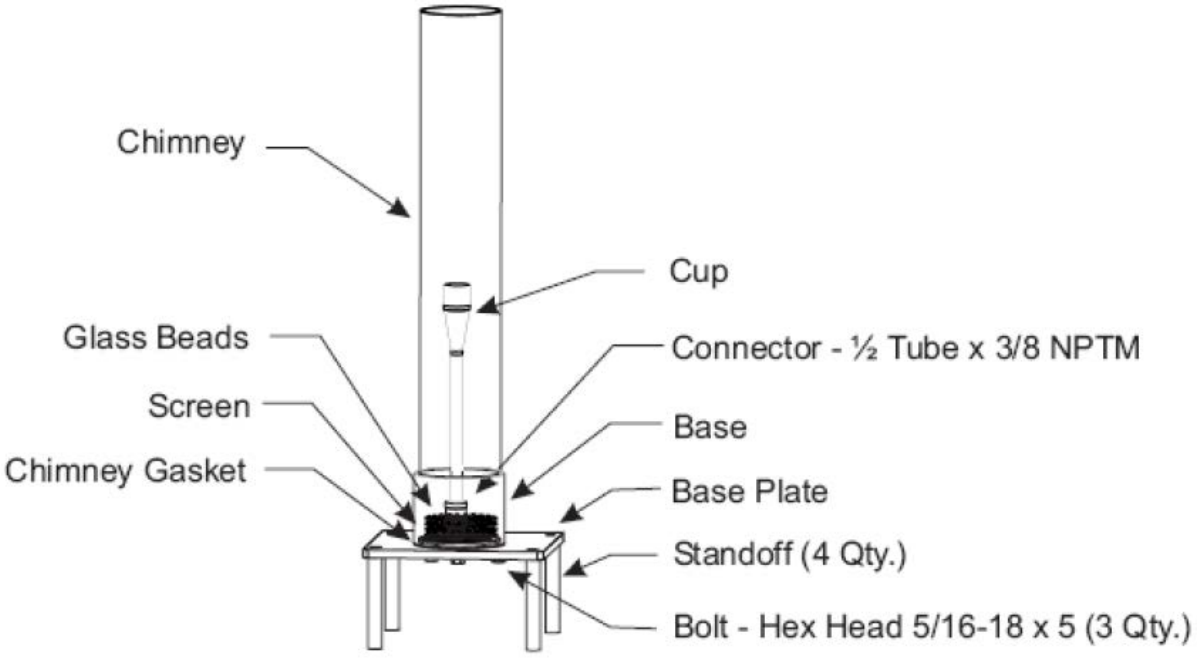

Figure 8. Illustration of the Cup Burner Apparatus
Source: Cup Burner Apparatus Manual by Kidde-Fenwal

The cup burner is typically used to study the effectiveness of an extinguishing agent. In a typical experiment, air is directed through the outer cylinder at a controlled flow rate of 40 L/min. The fuel is lit using an external igniter, which is then removed from the apparatus. Typically the fuel is a liquid, and flow controls are used to maintain the upper level of the liquid even with the rim of the cup. After a prescribed period of time, an extinguishing agent is added to the airflow in the outer cylinder and its effect on the burning fuel is noted. One useful application of the instrument is to determine the minimum concentration of an extinguishing agent necessary to extinguish the fuel. In a similar procedure, we have used the cup burner instrument to study the effect that oxygen (an accelerant) has upon burning fuel rather than an extinguishing agent. The procedures described in the Kidde-Fenwal cup-burner manual and NFPA 2001 Annex B "Cup-Burner Testing Method"[9] were followed, except as noted below to adjust for the differing goals of the experiment.

Evaluations were performed inside a 5- × 8-ft walk-in laboratory hood. During the experiment the exhaust system was turned off to ensure still air in the hood. All experiments were videotaped using a digital video camera capturing footage at a rate of 30 frames/s.

Cole-Parmer mass flow controllers were used to control the flow from compressed air and oxygen cylinders through the outer cylinder of the cup burner apparatus. A total air flow of 40 L/min was used for every test. Measurements were performed in atmospheres ranging from 100 percent air + 0 percent oxygen to 0 percent air + 100 percent oxygen in steps of 10 percent. Thus a total of eleven tests were performed for each fuel and fuel mixture studied. The total oxygen present is then:

$$\text{Total Oxygen Fraction} = 0.21 \times \chi_{\text{Air}} + 1.00 \times \chi_{\text{Oxygen}}$$

Where χ_{Air} is the fraction of air in the outer cylinder and χ_{Oxygen} is the fraction of oxygen. The use of actual compressed air rather than simulated air (i.e. mixed oxygen and nitrogen gasses) is recommended by the Kidde-Fenwal and NFPA documentation because compressed air contains trace gasses such as carbon dioxide and argon that can affect the combustion properties of the fuel.

Fuel samples and mixtures were prepared as described in Section 3.1 of this report covering the flame propagation testing. In no case was the fuel pre-heated for the cup burner experiments.

The fuel level in the inner cylinder cup was maintained by connecting the fuel inlet of the cup burner apparatus to the outlet of a 500-mL separatory funnel placed upon a vertical stage with a length of flexible Tygon tubing. The fuel level could then be maintained by raising and lowering the vertical stage, since gravity would cause the fuel level in the cub-burner to equal the fuel level in the funnel. Figure 9 shows the separatory funnel and vertical stage used for this procedure.

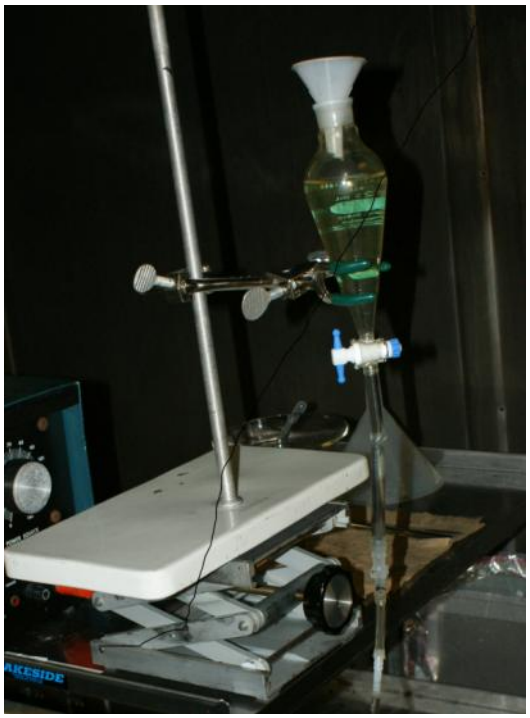

Figure 9. Separatory Funnel used to Control the Fuel Level

Before lighting, the fuel level was adjusted to 0.5 in below the rim of the cup. The fuel was then ignited in the cup using a heated coil of Nichrome wire suspended on the end of a metal rod. The rod and coil were removed from the cup-burner immediately after lighting the fuel. The fuel level was then raised as close to the rim of the cup as could be obtained without overflowing the cup.

The light intensity produced by the burning fuel in the cup-burner was measured using a Extech model EA33 digital light meter. The meter was mounted such that the light sensor was 1 in above the cup rim and 12.5 in horizontally distant from the outer quartz cylinder of the cup-burner apparatus. Note that elevated oxygen tests produced a considerable amount of heat and would likely have damaged the light sensor had it been stationed closer to the cup-burner.

Each cup-burner test was permitted to burn for a minimum of five minutes. Figure 10 shows a test involving burning JP-8 in a 50 percent air + 50 percent oxygen atmosphere.

Figure 10. Cup-Burner Test of JP-8 Performed in a 50% Air + 50% Oxygen Atmosphere

During the course of the test the operator had to be careful to maintain the fuel level at the proper level, since the flame size and emitted light intensity was strongly influenced by the fuel level. Allowing the fuel level to drop below the cup level reduced the flame size and light intensity considerably, while overflowing the cup caused a bright flare of burning fuel to form on the side of the cup, and invalidated the test according to the Kidde-Fenwal and NFPA procedures. During the test, as fuel was being consumed in the cup, the operator had to slowly raise the fuel level to compensate. This was somewhat offset in the first few minutes of the test by thermal expansion of the fuel which caused the fuel level to rise.

At the conclusion of the test the flow of compressed air and oxygen was terminated and compressed nitrogen was directed into the cup-burner to extinguish the flame.

3.3. Optical Flame Detection

Commercial OFDs were evaluated for their ability to detect HRJ and SPK fuel fires as compared to their ability to detect JP-8 fires. Nine flame detectors that utilize three IR sensors were evaluated (shown in Figure 11). Each detector has a unique sensitivity to jet fuel fires, so no detector results were compared to other detector results. Data was also collected from some single and multispectral detectors that were already installed in the facility and typically have less sensitivity to fuel fires. Table 1 lists the detectors evaluated in alphabetical order.

Table 1. Flame Detectors Tested

Manufacturer	Model	Sensor Type
Det-Tronics	X3301A very high	3-IR
Fire Sentry	FS24X	3-IR
General Monitors	FL4000	3-IR
Honeywell	FD-HA-IR3S-AD-X	3-IR
Net Safety	IR3S-A	3-IR
Spectrex	20/20I	3-IR
Spectrex	40/40I	3-IR
Spectronics	UVIR63	3-IR
Thorne Security	S231it	3-IR

Flame detection times were recorded for each detector from 2- × 2-ft and 1- × 1-ft pan fires located at three different distance/angle combinations (Table 2). These detector locations, relative to the fire, were chosen based on the typical detection distances for triple IR detectors. Although evaluations were performed similar to FM approval tests, results cannot be used as a basis of rating for the detectors.

Table 2. Flame Detection Distance/Angle Combinations

Distance	Angle	Pan size
210 ft	0°	2 × 2 ft
150 ft	45°	2 × 2 ft
150 ft	0°	1 1 ft

The fuel was ignited with a handheld propane torch. To ensure that the flame detectors did not respond to the torch, a shield was placed between the detectors and the fire during ignition. Once the fire was self sustaining and the surface of the pan was fully involved in flame, the shield was removed exposing the detectors to the flame.

Time was measured from when the shield was removed until each flame detector alarmed. A detector alarm was indicated when a red incandescent lamp mounted above each detector illuminated. All times for each detector were documented and verified by reviewing video recordings. The video recorded 30 frames/s, and the times for each sensor alarm were rounded up to the next highest second.

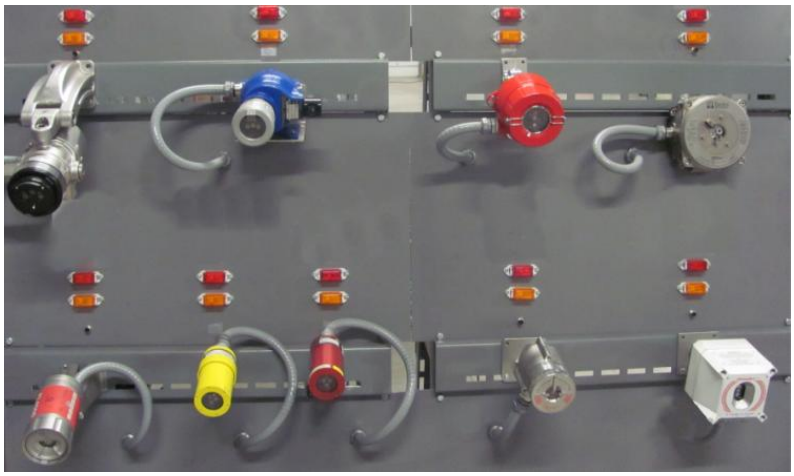

Figure 11. Triple-IR Sensor Detectors

Data was analyzed by comparing the means (averages) of the times to detection for the trials with JP-8 and for the combined trials with all the synthetic fuels and blends as unpaired samples. For each of the nine detectors the average time to detection when the fuel was JP-8 and the average time to detection when the fuel was synthetic or a blend (all fuels besides JP-8) were compared by dividing the difference in averages by the pooled variance to calculate a t-statistic. Differences in the averages were considered significant if the t-value was greater than or equal to the 97.5-percent confidence value. This analysis was repeated for each of the detectors and each of the three test conditions.

In addition to flame detection measurements, data was also collected on how many counts per second were recorded by UV and IR sensors. Counts are measurements of energy collected by an optical flame sensor. Counts per second are a typically used threshold in optical flame detectors that indicate the presence of a flame. This data can be used to determine the likelihood that a flame can be detected or to adjust OFD thresholds to ensure flame detection. Emissions from each fuel were measured in a 1- × 1-ft pan from 100 ft. The data was collected using a Det-Tronics UV/IR detector and software (Figure 12). The UV spectral sensitivity was 1850–2450 Å and the IR spectral sensitivity was 4.45 µm. Results are listed in Appendix B.

Figure 12. UV/IR Data Collection

3.4. Combustible Gas Detectors

HRJ and F-T SPK fuels, and blends of each, were evaluated to determine whether fuel vapors can be detected by USAF approved combustible gas indicators, also known as an explosive meter or LEL meters. In addition, correction factors or response factors for each fuel and JP-8 were determined. This effort will ensure safety of personnel that will work in areas that have potential for explosive fuel vapor buildup. The RAE Systems Inc. MultiRAE Plus and the MSA Sirius™ detectors were evaluated with JP-8 and alternative fuels. The MultiRAE Plus is no longer manufactured, and according to the manufacturer, the new detector product, called MultiRAE Family, has the same PID detection properties as the MultiRAE Plus.

The correction factor or response factor is a measurement of the relative measurement performance of the detector as compared to a standard or calibration gas such as isobutylene. This information is used to adjust the instrument's reading from the calibration gas concentration to the concentration of the gas being measured. The detector manufactures RAE Systems, Inc. and MSA agreed to perform evaluations in their respective laboratories to determine correction factors for each fuel. This data will be available for use with these alternative fuels for future operations.

The correction or response factor is determined by placing a known quantity of the individual fuel or fuel blend into a closed, known-volume container. This allows the concentration of the fuel to be calculated. The fuel is given time to evaporate and for vapors to equilibrate with the air in the container. The detector is calibrated with a known gas and the detector input port is then attached to the container and a fuel reading is obtained. This fuel reading is used to calculate the correction or response factor based on the known values of the calibration gas concentration, the calibration gas reading, the fuel concentration and the fuel reading [10]. Molecular weights of each fuel were required for this analysis. Appendix A describes the procedure for determining the fuel molecular weight.

4. RESULTS AND DISCUSSION

The fuels evaluated are a mixture of several components and each fuel has a balanced distribution of carbon numbers, similar to JP-8. They were made to have very similar properties to JP-8 such as boiling range, molecular weight range, flash point, freeze point, and vapor pressure. To confirm the properties of the fuels provided for use in these evaluations, some laboratory measurements and gas chromatography/mass spectrometry (GC/MS) analysis were conducted.

Camelina and Tallow HRJ samples were evaluated by GC/MS. The chromatogram for each is shown in Figure 13 with normal paraffins labeled by carbon number. Both samples were tested for flash point and density. Measured flash points were 105.8 °F for Camelina HRJ and 122 °F for Tallow HRJ. Density is listed in Table 3 along with boiling point ranges, flash points, and molecular weights of JP-8 and each of the alternative fuels/blends. The densities and boiling point ranges data were compiled from laboratory measurements and from Material Safety Data Sheets (MSDS). The method of obtaining the weighted average molecular weights is explained in Appendix A. The flash point test was conducted per ASTM D93-07 “Standard Test Methods for Flash Point by Pensky-Martens Closed Cup Tester”.

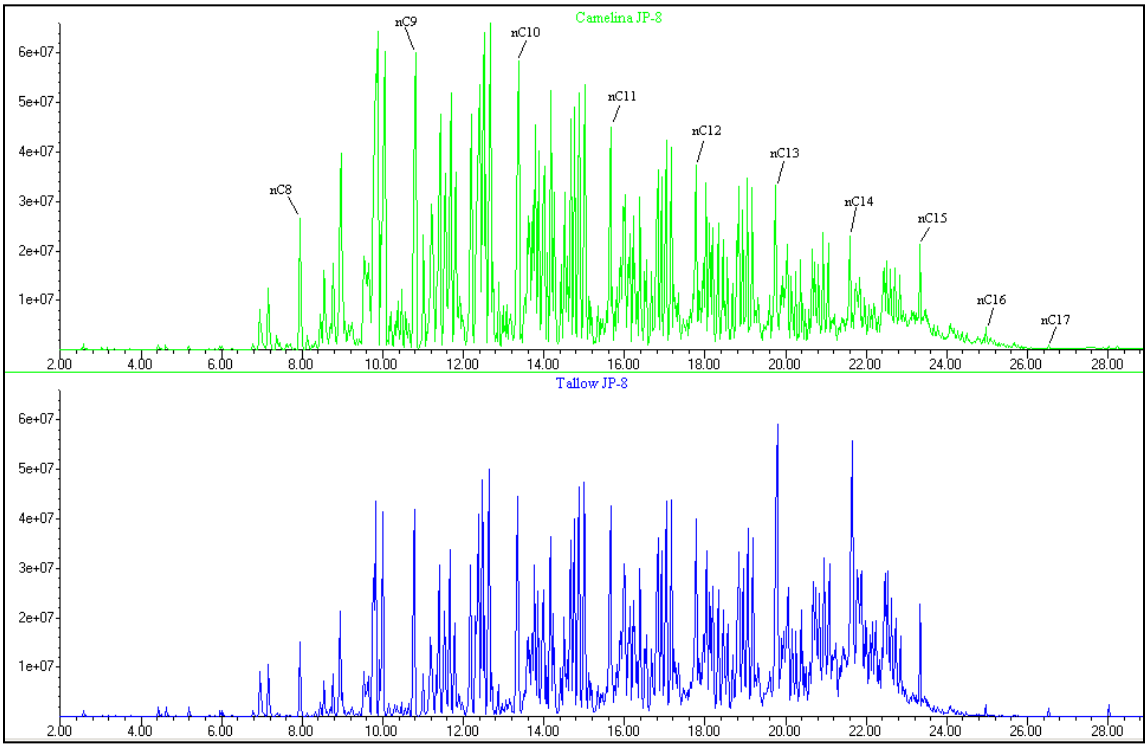

Figure 13. Camelina and Tallow GC/MS Chromatograms

Table 3. Fuel Properties

Fuel	Density lbs/ft^3 (kg/m^3)	Boiling Point °F	Flash Point °F	Average Molecular Weight g/mol
JP-8	50.44 (808)	360-471	129 (measured) >100 (MSDS)	158
Camelina HRJ	46.89 (751.2)	298-572	106 (measured) >100 (MSDS)	156
Camelina HRJ/JP-8 50/50	48.67 (779.6)	298-572	Not measured	154
Tallow HRJ	47.28 (757.4)	298-572	122 (measured) >100 (MSDS)	169
Tallow HRJ/JP-8 50/50	48.86 (782.7)	298-572	Not measured	161
Shell SPK	45.95 (736)	309-383	102-104 (measured) 100 (MSDS)	143
Shell SPK 50/50	48.25 (773)	320-457	Not measured	148

4.1. Flame Speed Propagation

Average flame spread rates were been measured for each fuel and fuel mixture at temperatures ranging from below to above the fuels flash point. A similar pattern was observed for all fuels and fuel mixtures over the temperature ranges studied in this project. The flame propagation rates were approximately constant, on the order of 5 to 10 in/s, from room temperature to just below the fuel's flash points. The flame propagation rate then increased rapidly over a range of approximately 20 to 30 °F until a maximum value on the order of 55 to 65 in/s was reached. From that point on the flame propagation rates were approximately constant, up to the maximum temperatures tested. An idealized plot of temperature vs. flame propagation rate for a hypothetical fuel which displays these trends is presented in Figure 14.

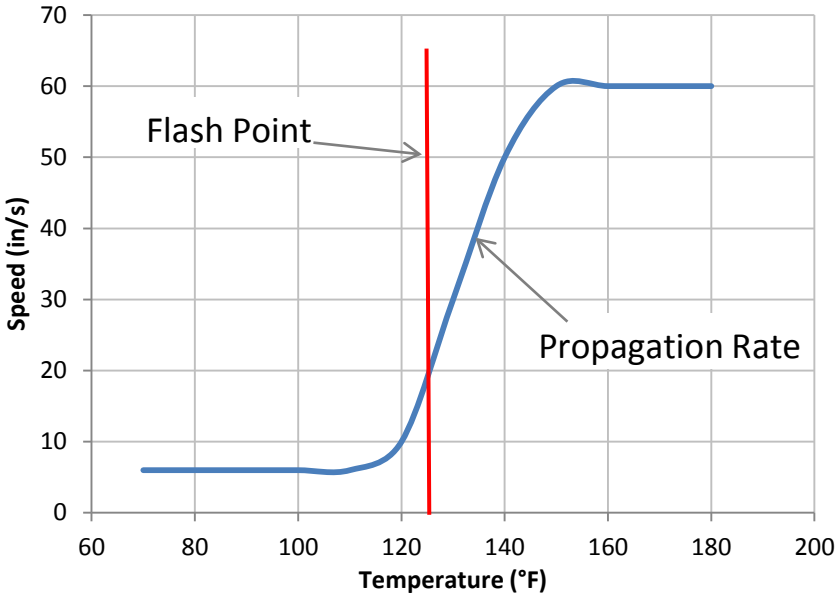

Figure 14. Idealized Flame Propagation Rate Plot for a Hypothetical Fuel

Figure 15 presents the measured flame propagation rates for JP-8, Camelina HRJ, Tallow HRJ, and Shell SPK fuels. All fuels had similar flame propagation rates at low and high temperatures. Shell SPK and Camelina HRJ fuels, which had the lowest flash points, had the lowest temperature transition from low to high flame propagation rate regions. Similarly, JP-8, which had the highest flash point, had the highest temperature transition from the low to high flame propagation rate region.

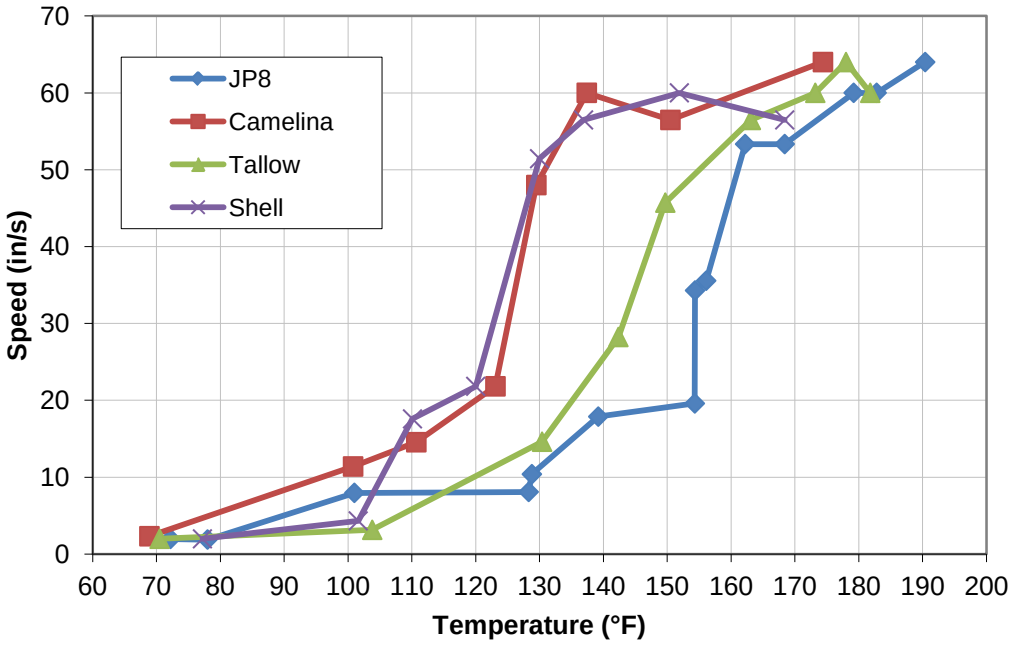

Figure 15. Flame Propagation Results for Pure Fuels

Figure 16 through Figure 18 present the measured flame propagation rate for JP-8, the three synthetic fuels, and 50/50 mixtures of JP-8 and the three synthetic fuels. In all cases the flame propagation rates of each 50/50 mixture falls between the flame propagation rate of pure JP-8 and the respective pure synthetic fuel.

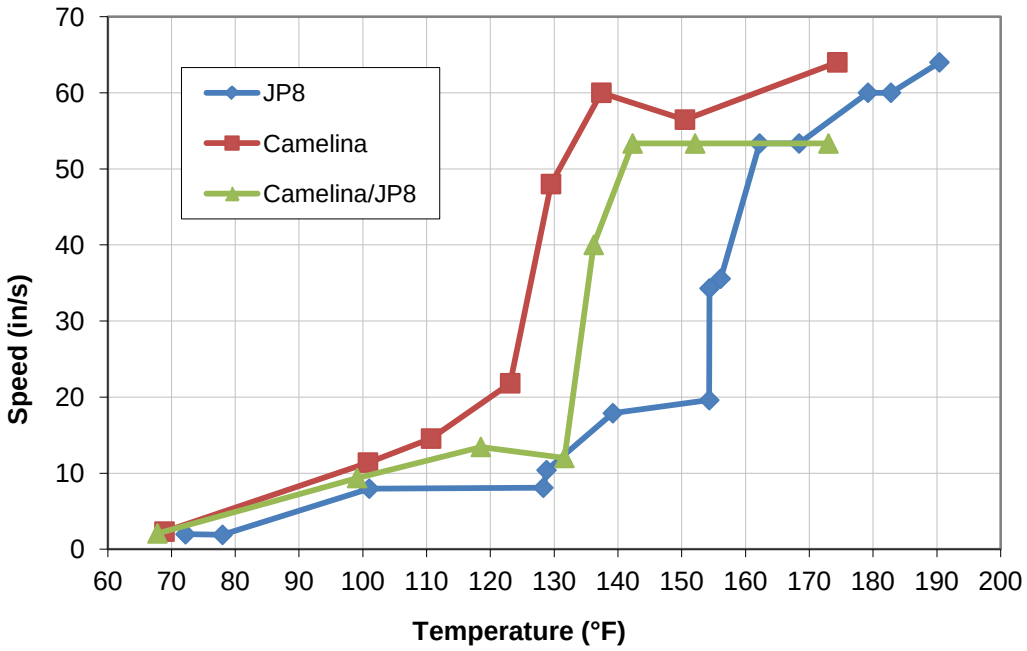

Figure 16. Flame Propagation Results for JP-8, Camelina, and a 50/50 Mixture of JP-8 and Camelina

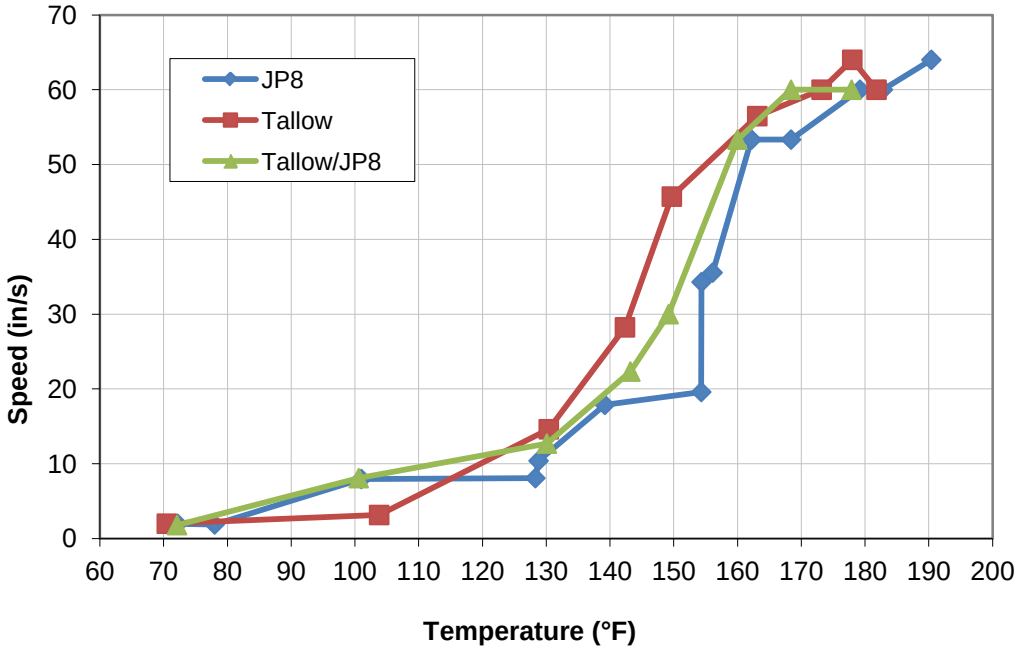

Figure 17. Flame Propagation Results for JP-8, Tallow, and a 50/50 Mixture of JP-8 and Tallow

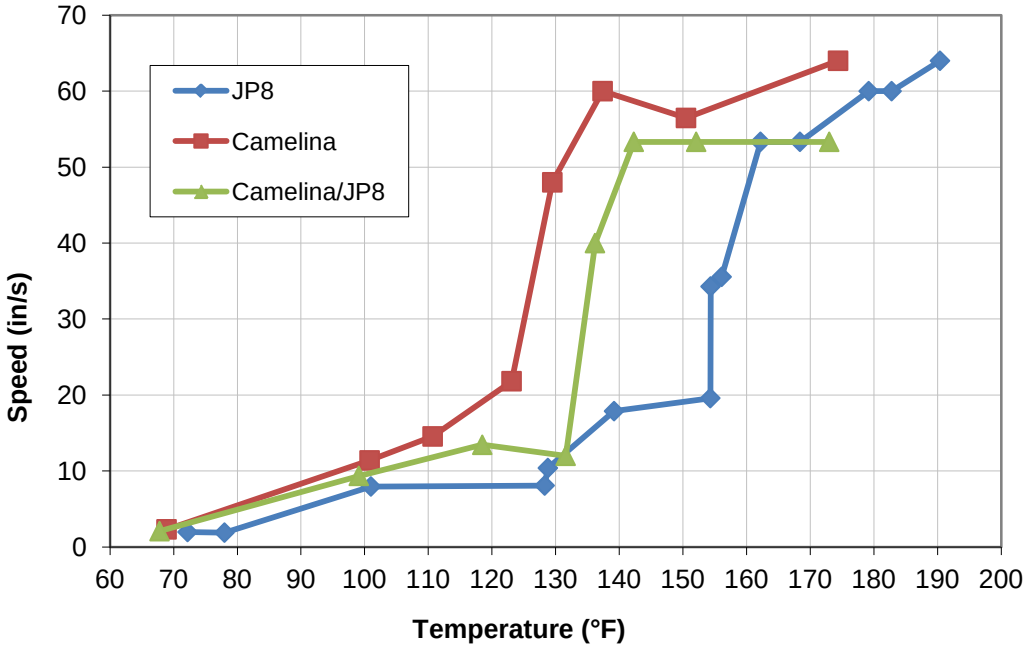

Figure 18. Flame Propagation Results for JP-8, Shell, and a 50/50 Mixture of JP-8 and Shell

4.1.1. Soot Production Analysis

Six typical photomicrographs from the soot production analysis are shown in Figure 19, below. These images are all from sticky-pad collections, exposed sticky-side up to the test fire and then affixed to the bottom of a clean microscope slide. The upper two images are the lowest (left) and

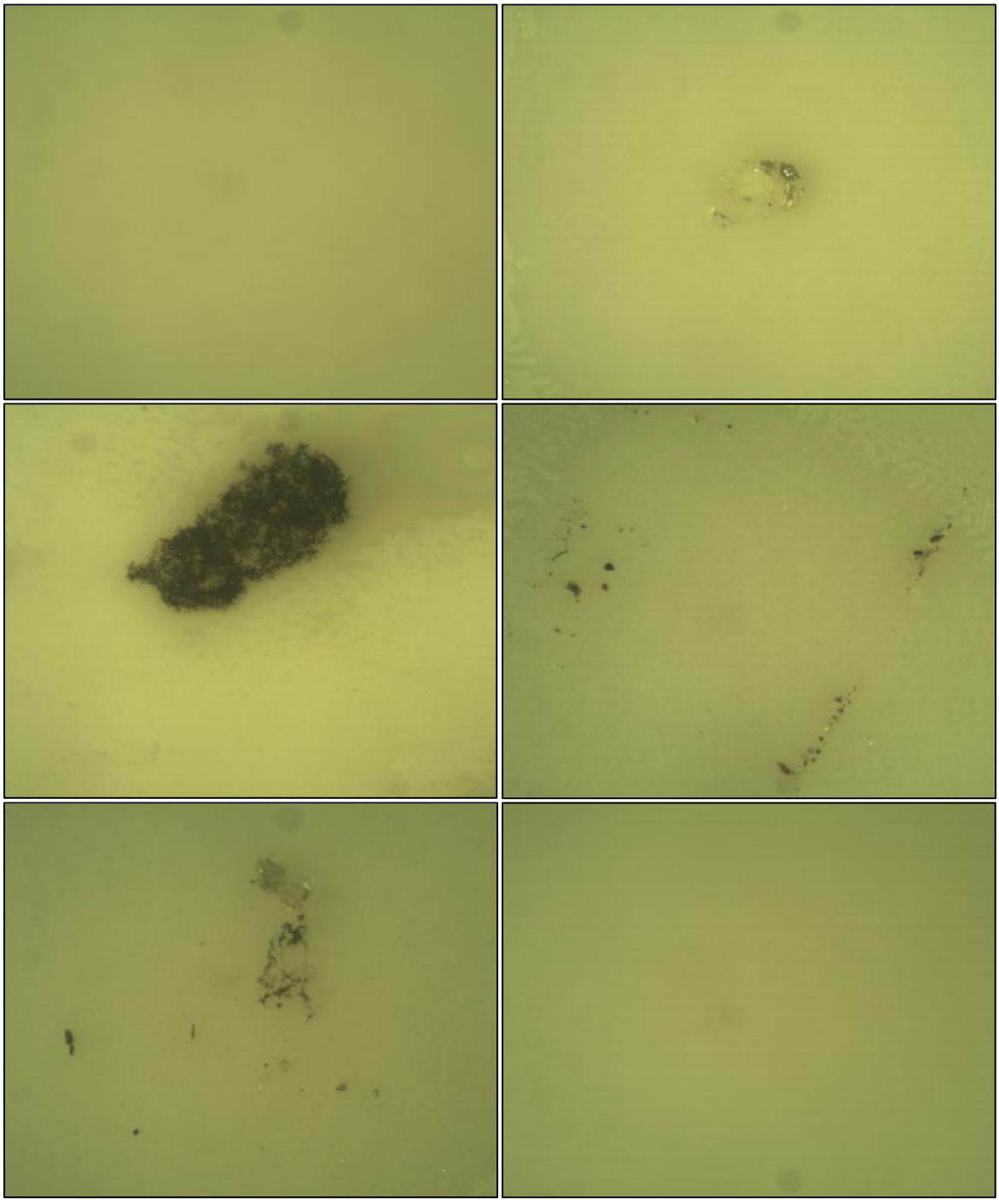

Figure 19. Photomicrographs of Smoke Particles Trapped with White Sticky Pad Media

highest particle counts from a blank or un-exposed sticky pad. The second row of images are the highest particle count from JP-8 (left) and Shell SPK (right). The third row of images are the highest particle count from Camelina HRJ (left) and Tallow HRJ (right).

The actual particulate catches for each fuel varied widely. There were some results to suggest the aluminum foil might have caught more particles, but particles were also observed to blow off of aluminum foil substrates when moving them out of the hood to the adjacent laboratory bench. Similar secondary movement of particles was observed from the white copy/printer paper substrates. Accordingly the results reported in Table 4 below are for the sticky-pad collections.

Table 4. Summary of Results from Sticky-pad Colleciton of Smoke Particles

Sticky-Pad Collection Data Summary				
	Fuel Type			
	JP-8	Shell SPK	Camelina HRJ	Tallow HRJ
Overall Mean:	3.12E+04	3.99E+03	5.11E+03	1.36E+02
Stdev:	4.86E+04	4.98E+03	5.74E+03	4.02E+02
Min:	1.32E+03	7.84E+01	4.10E+02	0.00E+00
Max:	2.12E+05	2.08E+04	2.59E+04	1.97E+03
Median:	1.37E+04	2.11E+03	3.11E+03	0.00E+00
Number of Fields of View:	21	31	25	29
Number of Sticky Sheets:	2	3	3	3

The numbers for mean and standard deviation represent the area of smoke particle coverage of the microscopic field of view, in terms of pixels. Separate measurements have shown the microscope and camera system produced pixels of a size of 2.02E-05 in in length. The overall field of view from each observation was 1280 × 1024 pixels or 1.3107×10^6 pixels.

The smoke particles in this effort were measured as settled smoke particles. JP-8 fuel produced the largest collection of smoke particulates as measured by the average (mean) collection, producing an order of magnitude larger settled smoke concentration. Tallow HRJ-8 produced the smallest collection of settled smoke particulates. Shell SPK and Camelina HRJ produced intermediate amounts of settled smoke particulates. The overall order of measurements for settled smoke particulates was JP-8 > Camelina HRJ > Shell SPK > Tallow HRJ.

A somewhat different indirect smoke production measure was used during an independent study of suppression of flames. The alternative approach used the flame luminosity, as analyzed by MATLAB® from digital photographs of fuel fires. JP-8 in this independent estimate was found to produce much larger amounts of smoke than Camelina HRJ and Tallow HRJ, but the measurements for Camelina HRJ and Tallow HRJ were closely similar. In the measurement of smoke from flame luminosity, the order was JP-8 > Tallow HRJ ≈ Camelina HRJ.[11]

A more rigorous measurement of smoke particulate production from fires as a function of the fuel used would require collection and gravimetric analysis of smoke particles from representative test fires. Instrumental smoke monitoring could also be used.

4.2. Flame Visible Spectrum Emissions

4.2.1. Light Intensity

Analysis of the light intensity measurements was somewhat difficult due to the variance in emitted light levels observed over the course of each test. During each cup-burner test, the light emitted by the burning fuel varied over a large range due to several factors:

- The light intensity dropped rapidly if the fuel level was allowed to drop below the rim of the cup. Thus it was necessary for the operator to continually raise the fuel level to compensate for fuel lost due to combustion. This was especially important at higher oxygen concentrations where fuel was consumed at a much higher rate.
- During the test, soot would accumulate on the side of the outer quartz cylinder of the cup-burner apparatus which would reduce the light intensity seen by the digital light meter outside the cylinder.
- The visible flame had a natural tendency to vary over time even when fuel levels and airflows were held as constant as possible. The measured light intensity often varied considerably over the course of a few seconds.

Because of these factors it would be inappropriate to simply report the average light level observed during the course of the experiment. We have instead chosen to identify and report the maximum light intensity value that was sustained for a period of one second or longer for each fuel at each atmospheric composition. This eliminates the very short, bright flashes of light that were frequently observed as well as the periods when the operator inadvertently allowed the fuel level to drop resulting in low light intensity.

Figure 20 presents the maximum sustained light intensity observed for JP-8, Camelina HRJ, Tallow HRJ, and Shell SPK. At normal atmospheric conditions, the JP-8 produced a light intensity of 37 Lux, while the three synthetic fuels were somewhat higher, ranging from 44 to 46 Lux. Emitted light intensity increased with increasing oxygen content for all fuels. Under pure oxygen conditions, JP-8 produced a light intensity of 480 Lux, while the three synthetic fuels ranged from 610 to 820 Lux. The three synthetic fuels produced higher light intensities than JP-8 at all oxygen concentrations.

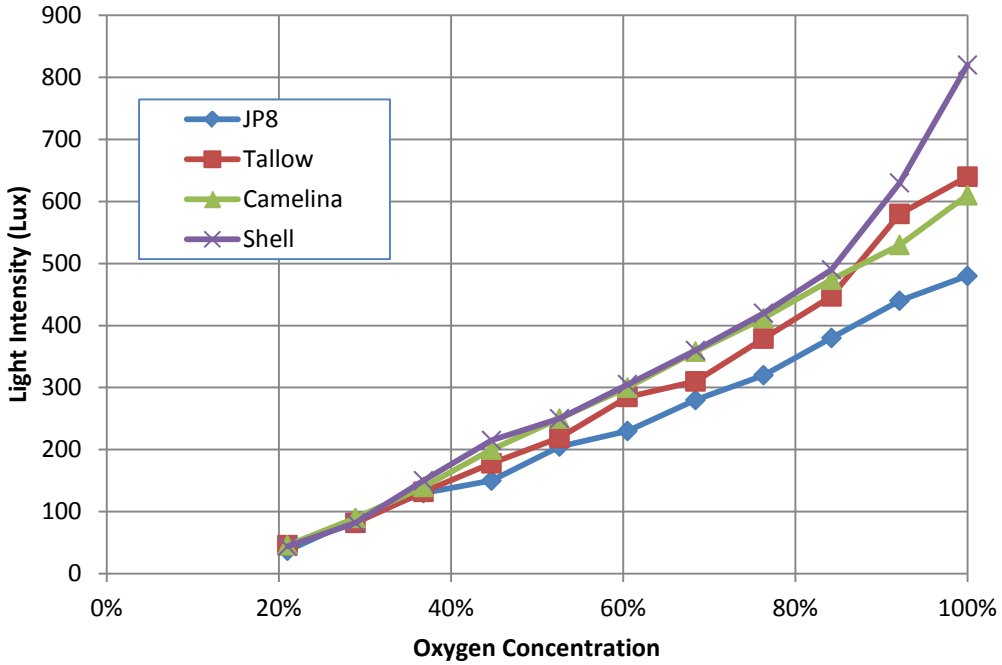

Figure 20. Visible Emission Results for Pure Fuels

Figure 21 through Figure 23 present the maximum sustained light intensity for JP-8, the three synthetic fuels, and 50/50 mixtures of JP-8 and the three synthetic fuels. In all cases the light intensity of each 50/50 mixture generally falls between the light intensity of pure JP-8 and the respective pure synthetic fuel.

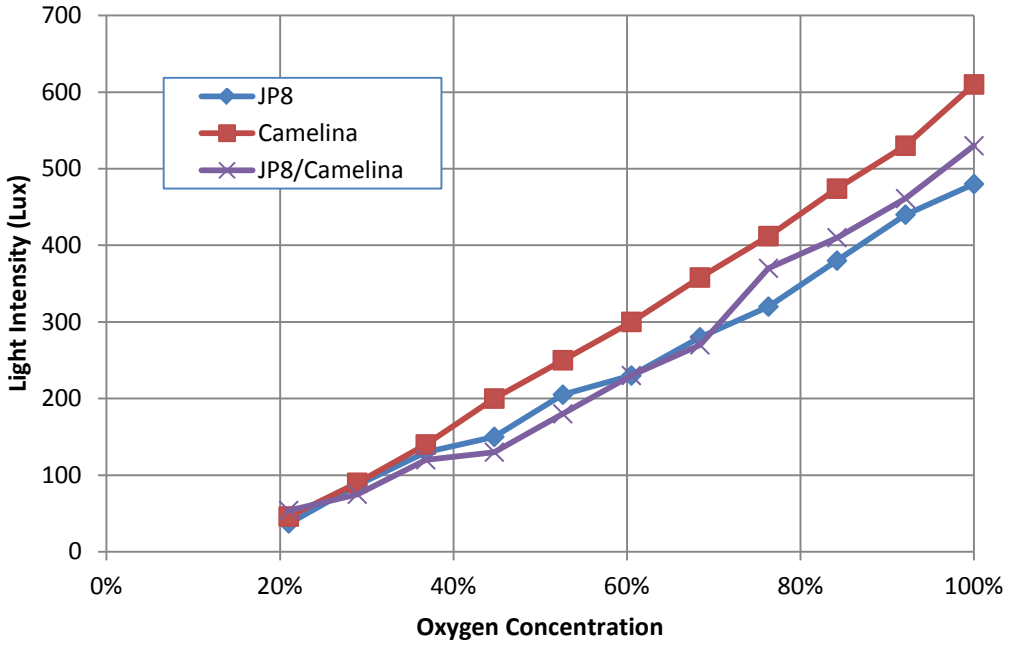

Figure 21. Visible Emission Results for JP-8, Camelina, and a 50/50 Mixture of JP-8 and Camelina

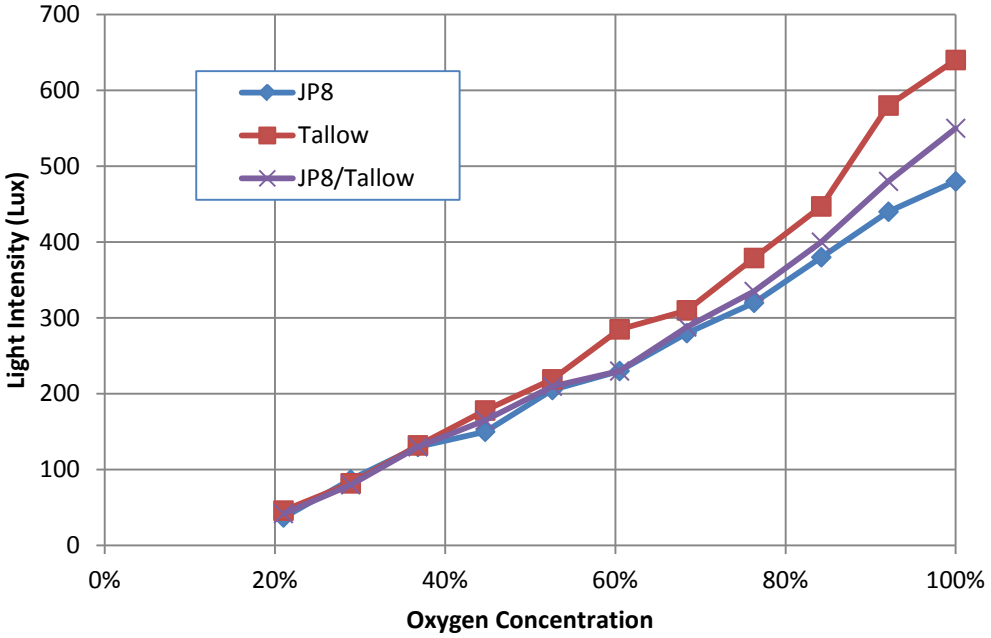

Figure 22. Visible Emission Results for JP-8, Tallow, and a 50/50 Mixture of JP-8 and Tallow

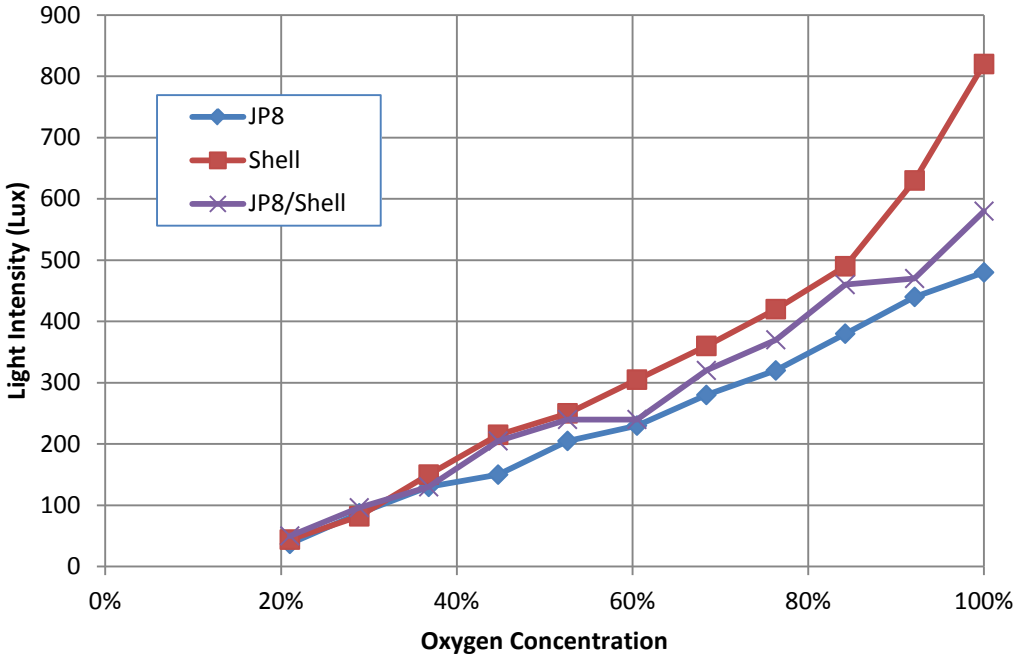

Figure 23. Visible Emission Results for JP-8, Shell, and a 50/50 Mixture of JP-8 and Shell

4.2.2. Flame Temperature

Initial attempts were made to measure the flame temperature during the cup-burner experiments by using a type K thermocouple suspended one inch above the center of the cup during the test. Temperatures recorded during tests in pure air were essentially the same for all fuels studied.

Flame temperatures measured in increased oxygen atmospheres were significantly higher. At oxygen concentrations above 40 percent the flame temperature became hot enough to destroy the thermocouple. Due to these difficulties, we did not attempt further measurements of the flame temperature and this data remains incomplete and inconclusive at this point.

4.2.3. Soot Generation

It was noted that less soot was generated and deposited on the cup-burner apparatus when performing tests at higher oxygen concentrations compared to lower oxygen concentration tests. It is likely that the higher flame temperatures and higher oxygen concentrations resulted in more complete combustion of the fuels in those cases. Similarly, it was noted that less soot was generated when performing tests on the three synthetic fuels than when performing test on JP-8. This may have been due to differences in the chemical composition of the fuels. It is likely that the synthetic fuels had greater oxygen content in the form of alcohols, ethers, and other oxygen containing functional groups which would promote more complete combustion of the fuel. Similarly, it is likely that the JP-8 contained a greater concentration of aromatic hydrocarbon compounds and sulfur containing compounds that would be more difficult to combust. No attempt was made to quantify the soot generated during these tests.

4.3. Optical Flame Detection

As discussed in Section 3.3, an array of flames detectors was subjected to radiation from JP-8 and alternative fuel fires from three different distance/angle/pan size combinations based on the typical detection distances for triple IR detectors. Figure 24 shows a typical 1-ft by-1 ft pan fire. In the data presented below, each detector is represented by a letter, A through I.

Figure 24. 1-ft × 1-ft Pan Fire

4.3.1. 2- × 2-ft pan fire - 210 ft - Angle 0°

The array of flame detectors was placed 210 ft from the 2- × 2-ft fire pan. The detectors were aimed directly at the pan at a 0° angle. The results are listed in Table 5. Each row in the table indicates a single pan fire. Seven of the nine detectors detected all of the JP-8 fires within 30 s, and eight of the nine detectors detected all of the alternative fuel and fuel blend fires within 30 s.

Many response times measured for the alternative fuel and fuel blend fires were equivalent to or faster than for JP-8 fires. Two of the detectors responded to every fire within 10 s.

Table 5. Flame Detection Times (s); 2- × 2-ft, 210 ft, 0°

	Triple IR Detectors								
FUEL	**A**	**B**	**C**	**D**	**E**	**F**	**G**	**H**	**I**
JP-8	3	15	8	26	13	5	DN	3	4
JP-8	5	3	13	30	16	11	DN	8	4
JP-8	6	18	12	33	16	7	DN	7	8
Camelina	3	3	7	12	4	4	DN	7	6
Camelina	4	5	14	21	8	7	DN	10	7
Camelina 50/50	3	4	11	13	8	10	DN	8	5
Camelina 50/50	3	13	13	14	19	8	DN	10	5
Tallow	5	18	8	13	9	6	DN	7	5
Tallow	3	9	11	13	11	11	DN	11	7
Tallow 50/50	2	24	14	13	19	16	DN	11	8
Tallow 50/50	3	11	12	19	19	7	DN	10	10
Shell	2	14	8	13	6	4	DN	7	4
Shell	2	7	7	14	11	11	DN	16	4
Shell 50/50	3	7	6	19	5	5	DN	7	6
Shell 50/50	3	9	7	16	7	6	DN	5	9

DN- Did not detect

Treating the test as an unpaired design to compare detector response times for each detector to JP-8 and to the synthetic fuels and blends, comparison of the average detection times showed that all of the detectors were as good or better at detecting flames from synthetic fuels and blends of synthetic fuel and JP-8 than they were at detecting flames from JP-8 alone.

4.3.2. 2- × 2-ft Pan Fire - 150 ft - Angle 45°

The array of flame detectors was placed 150 ft from the 2- × 2-ft fire pan. The detectors were aimed 45 degrees from the centerline view of the detectors. The results are listed in Table 6. Four of the nine detectors detected all of the JP-8 fires within 30 s, and five of the nine detectors detected most of the alternative fuel and fuel blend fires within 30 s. The other four detectors did not detect these fires due to reasons such as their sensitivity and field-of-view.

Table 6. Flame Detection Times (s); 2- × 2-ft, 150 ft, 45°

	Triple IR Detectors								
FUEL	**A**	**B**	**C**	**D**	**E**	**F**	**G**	**H**	**I**
JP-8	DN	24	9	DN	DN	DN	DN	10	7
JP-8	DN	9	13	DN	DN	DN	DN	12	8
JP-8	DN	7	12	DN	DN	DN	DN	6	8
Camelina	DN	10	9	13	DN	DN	DN	16	8
Camelina	DN	6	7	13	DN	DN	DN	11	7
Camelina 50/50	DN	7	11	DN	DN	DN	DN	13	7
Camelina 50/50	DN	4	9	39	DN	DN	DN	8	6
Tallow	DN	4	13	13	DN	DN	DN	19	8
Tallow	DN	5	10	15	DN	DN	DN	23	5
Tallow 50/50	DN	5	10	18	DN	DN	DN	7	8
Tallow 50/50	DN	3	12	DN	DN	DN	DN	12	11
Shell	DN	5	7	13	DN	DN	DN	15	6
Shell	DN	4	6	13	DN	DN	DN	8	7
Shell 50/50	DN	9	9	DN	DN	DN	DN	33	6
Shell 50/50	DN	4	8	14	DN	DN	DN	16	5

DN- Did not detect

Comparison of the average detection times for flames from JP-8 and for flames from the synthetic fuels and blends showed that all of the detectors were as good or better at detecting flames from synthetic fuels and blends of synthetic fuels and JP-8 than they were at detecting flames from JP-8 alone.

4.3.3. 1- × 1-ft Pan Fire - 150 ft - Angle 0°

The array of flame detectors was placed 150 ft from the 1- × 1-ft fire pan. The detectors were aimed directly at the pan at a 0° angle. The results are listed in Table 7. Five of the nine detectors detected all of the JP-8 fires within 30 s, and seven of the nine detectors detected all of the alternative fuel and fuel blend fires within 30 s.

Table 7. Flame Detection Times (s); 1- × 1-ft, 150 ft, 0°

	Triple IR Detectors								
FUEL	**A**	**B**	**C**	**D**	**E**	**F**	**G**	**H**	**I**
JP-8	3	5	26	56	47	19	DN	16	5
JP-8	5	7	35	40	29	7	DN	14	6
Camelina	4	8	7	13	7	4	DN	29	5
Camelina	10	14	16	13	18	4	DN	15	7
Camelina 50/50	2	4	13	13	1	1	DN	15	7
Camelina 50/50	4	11	16	15	13	2	DN	12	8
Camelina 50/50	5	31	27	14	13	13	DN	21	9
Tallow	3	20	14	13	13	5	DN	18	5
Tallow	3	29	15	13	7	7	DN	16	6
Tallow 50/50	3	6	18	14	14	14	DN	11	5
Tallow 50/50	2	9	13	14	11	5	DN	10	9
Shell	4	8	5	13	9	6	DN	11	7
Shell	4	8	10	14	15	5	DN	12	6
Shell 50/50	10	4	8	14	3	6	DN	7	6
Shell 50/50	11	12	16	14	10	13	DN	15	5

DN- Did not detect

Comparison of the average detection times for flames from JP-8 and for flames from the synthetic fuels and blends showed that all of the detectors were as good or better at detecting flames from synthetic fuels and blends of synthetic fuels and JP-8 than they were at detecting flames from JP-8 alone.

4.4. Combustible Gas Detectors

4.4.1. MSA Detector Results

MSA uses the term “response factor” to designate the multiplier used to adjust a CGD reading from the gas to which it is calibrated to the gas being measured. A Sirius® Multigas Detector was used to measure the response factors of each of the fuels and fuel blends relative to isobutylene. Five readings were averaged for each fuel. Table 8 has the results from the measurements. These data were provided by MSA.

Table 8. MSA PID Fuel Response Factors

FUEL	Mean Response Factor (10.6eV lamp)	std dev
JP-8	1.17	0.15
Camelina	0.95	0.10
Camelina 50/50	1.05	0.10
Tallow	1.29	0.15
Tallow 50/50	1.06	0.17
Shell	0.89	0.10
Shell 50/50	0.93	0.09

4.4.2. RAE Detector Results

RAE Systems uses the term “correction factor” to designate the multiplier used to adjust a CGD reading from the gas to which it is calibrated to the gas being measured. The MultiRAE Plus detector was used to measure the correction factors of each of the fuels and fuel blends relative to isobutylene. Table 9 has the results from the measurements for 10.6 eV PID lamps and for 11.7 eV PID lamps. These data were provided by RAE Systems.

Table 9. RAE Systems PID Fuel Correction Factors

FUEL	Correction Factor (10.6eV lamp)	Correction Factor (11.7eV lamp)
JP-8	0.85	0.42
Camelina	1.1	0.32
Camelina 50/50	0.89	0.4
Tallow	0.95	0.36
Tallow 50/50	0.9	0.39
Shell	1.29	0.4
Shell 50/50	1.07	0.41

5. CONCLUSIONS AND RECOMMENDATIONS

Significant safety issues with these alternative fuels, as compared to JP-8 fuel, did not emerge in these evaluations. Notable safety observations were that the temperature at which the flame propagation rate changes from low speed to high speed varied marginally in the fuels with flash point, no flame visibility issues were observed, and optical flame and combustible gas detectors will respond to these fuels or fires involving them.

5.1. Flame Speed Propagation

A similar pattern was observed for all fuels and fuel mixtures over the temperature ranges studied in this project. The flame propagation rates were approximately constant, on the order of 5 to 10 in/s, from room temperature to just below the fuel's flash points. The flame propagation rate then increased rapidly over a range of approximately 20 to 30 °F until a maximum value on the order of 55 to 65 in/s was reached. From that point on the flame propagation rates were approximately constant up to the maximum temperatures tested.

During the measurements of flame speed propagation, JP-8 fuel produced the largest collection of smoke particulates as measured by the average (mean) collection, producing an order of magnitude larger settled smoke particle concentration. Tallow HRJ produced the smallest collection of settled smoke particulates. Shell SPK and Camelina HRJ produced intermediate amounts of settled smoke particulates. The overall order of measurements for settled smoke particulates was JP-8 > Camelina HRJ > Shell SPK > Tallow HRJ.

5.2. Flame Visible Spectrum Emissions

The measured visible light intensity increased with increasing oxygen concentration for all fuels and fuel mixtures studied. The three synthetic fuels emitted higher light intensities that JP-8 at all oxygen concentrations. Measured light intensities for 50/50 mixtures of JP-8 and a synthetic fuel generally fell between the measured light intensify of JP-8 and the respective pure synthetic fuel. It was noted that flame temperatures increased and soot generation decreased with increasing oxygen concentration. It was also observed that the three synthetic fuels generated less soot that JP-8 under equivalent conditions.

5.3. Optical Flame Detection

Results show that the alternative fuels are capable of being detected by the commercially available flame detectors that are currently used to detect JP-8 fires without any modification to the detector logic. In some cases the alternative fuel fires were detected more quickly than JP-8 fires.

Based on the FM flame response sensitivity test requirements, it is believed that eight detectors that were evaluated have potential to meet the FM performance requirements for the alternative fuels and blends with 2- × 2-ft fires located at 210 ft. Two of the flame detectors stood out above the others in these evaluations. These two have potential to meet the FM performance requirements for the alternative fuels and blends with response times less than 10 s.

5.4. Combustible Gas Detectors

PID gas detectors are able to detect the HRJ fuels, HRJ fuel blends, SPK fuels, and SPK fuel blends. Correction factors or response factors were determined for each fuel.

6. REFERENCES

1. Lille, Simon; Blasiak, Wlodzimierz; Jewartowski, Marcin. *Experimental study of the fuel jet combustion in high temperature and low oxygen content exhaust gases*. Energy Volume 30, Issues 2-4, February-March 2005, Pages 373-384.

2. Gottuk, D.T., Scheffey, J.L., Williams, F.W., Gott, J.E., Tabet, R.J. *Optical Fire Detection (OFD) for Military Aircraft Hangars: Final Report on OFD performance to Fuel Spill Fires and Optical Stresses*. NRL/MR/6180--00-8457. 1999.

3. *American National Standard for Radiant-Energy Sensing Fire Detectors for Automatic Fire Alarm Signaling*. ANSI/FM Approvals 3260. February 2004.

4. Air Force Engineering Technical Letter (ETL) 02-15: *Fire Protection Engineering Criteria - New Aircraft Facilities*. http://www.wbdg.org/ccb/AF/AFETL/etl_02_15.pdf.

5. TO 1-1-3. *Inspection and Repair of Aircraft Integral Tanks and Fuel Cells*. 22 December 2009; Change 2 - 24 January 2011.

6. Air Force Manual 10-2507. *Readiness and Emergency Management (R&EM) Flight Operations*. 14 May 2009; Supplement 24 February 2011.

7. Wells, S.P., Cozart, K.S., Mitchell, M.B., Dodsworth R. D. *Aircraft Hangar Fire Threat Study and Analysis.* AFRL-ML-TY-TR-1998-4504. December 1997.

8. Mayfield, Howard T., Pickett, Brent M., and Shelley, Timothy J. *Firefighting and Emergency Response Study of Advanced Composites Aircraft. Objective 4: Post Fire Decontamination of Personal Protection Equipment*. AFRL-RX-TY-TR-2011-0071. November 2011.

9. National Fire Protection Association (NFPA) 2001, Standard on Clean Agent Fire Extinguishing Systems, 2012 Edition. Annex B “Cup-Burner Testing Method”

10. *Measuring PID Correction Factors for Volatile Compounds with RAE Systems Instruments*, Technical Note, TN-120, rev.2 wh. 11-04.

11. Wells, Steven, Pickett, Brent M., and Mayfield, Howard. *Evaluation of Suppression of Hydroprocessed Renewable Jet (HRJ) Fuel Fires with Aqueous Film Forming Foam (AFFF)*, AFRL-RX-TY-TR-2011-0101. July 2011.

Appendix A: Jet Fuel Effective Molecular Weight Estimation

A.1. BACKGROUND

The question of the molecular weight of jet fuels cannot be directly answered as all common jet fuels except special-purpose missile fuels are mixtures of a wide variety of organic compounds. Each substance in the mixture possesses its own molecular weight, and typical jet fuels will contain hundreds or thousands of organic compounds. One method to estimate an effective molecular weight for fuel samples is to perform a GC/MS analysis, calculate a weighted average molecular weight based on the peak relative area, and estimate molecular weight from the apex mass spectrum of each gas chromatographic peak.

The total ion chromatogram (TIC) is one possible result from a GC/MS analysis. GC/MS data are acquired as a series of mass spectra, recorded one-after-another over the course of an analysis run with the assistance of a data system computer. The TIC is obtained by summing the detector signal intensities for each mass spectrum and plotting the total ion intensity against the acquisition time when each mass spectral scan was started. The plot usually displays multiple peaks, each one indicating when a chemical compound has passed out of the gas chromatograph's separatory column and into the ion source of the mass spectrometer. The area under the curve of each peak in the plot can be obtained by integrating the peak, usually with numerical analysis software. The signal intensity of the TIC is directly related to the amount of the compound producing the mass spectral signals, and can thus serve as a quantitative measure for the amount of the compound present in the sample. The TIC is analogous to the signal obtained from a flame ionization detector (FID) as both are obtained by ionizing organic compounds. Both FID and a mass spectrometer can respond to all organic compounds, but a mass spectrometer is a more universal detector from its ability to respond to chemical compounds without carbon-carbon or carbon-hydrogen bonds. From both FID chromatograms and the TIC, a common practice is to use the data system computer to detect the peaks in the chromatogram (by way of signal analysis from the chromatogram trace), integrate the peak to obtain its area, and produce a report listing the retention time (the time the compound exited the chromatographic column), peak area, and the relative area of the peak expressed as a percentage of the total area. More sophisticated analyses are available to quantify a compound present in a sample from its peak area, but these procedures are more complicated and involve calibration with standard samples containing known concentrations of the compound of interest.

The GC/MS procedure separates a sample into component compounds according to their relative affinities for the stationary phase of the gas chromatographic column and according to their vapor pressure vs. temperature characteristics. As each compound's chromatographic band exits the column the material passes into the ion source of the mass spectrometer, forming ions and fragmenting according to the molecular structure and resulting in the mass spectrum by the scanning of the mass filter as a function of time. Analysis of the mass spectrum by human interpretation or computer library searching yields clues to the identity of unknown compounds present in the sample or confirms known components. Such analyses may also indicate the compound's molecular weight, either from the library database results from a library search or by human interpretation to find a molecular ion peak in the spectrum.

A.2. METHODS, ASSUMPTIONS, AND PROCEDURES

Four samples were evaluated for determination of effective molecular weight. These samples were a sample of Exxon Mobil JP-8, a sample of Shell SPK, a sample of Camelina HRJ, and a sample of Tallow HRJ. The samples were submitted for GC/MS analysis without extensive information as to their sources, methods of preparation, or history (batch number, etc). Laboratory personnel analyzed the samples by GC/MS and obtained a weighted average molecular weight, based on molecular weight estimates for each peak and the percent area of the peak in the TIC. This relationship is shown in Equation A-1, with M_w representing the weighted average molecular weight, M_i representing the molecular weight for peak *i*, and P_i representing the percentage area of peak *i*, for *n* peaks detected by the peak integration software in a sample's TIC.

$$\boldsymbol{M_w = \frac{\sum_{i=1}^{n} P_i M_i}{\sum_{i=1}^{n} P_i}} \qquad \text{(A-1)}$$

Molecular weights for the components could be estimated from the peak mass spectra in several ways. The mass spectrum considered to be most representative of the compound responsible for a given peak was the mass spectral scan taken at or nearest to the apex of each peak. Each mass spectrum was examined for evidence of a molecular ion peak, with the knowledge that many organic compounds' molecular ions fragment easily and extensively yielding weak molecular ion peaks or none at all. Each apex mass spectrum was also submitted for a computerized library search for 20 best matches from the Wiley Library[1]. Where the molecular ion was apparent to the human interpreter, its nominal mass was recorded as the molecular weight of the peak. Where the library search identified several promising mass spectra with the same molecular weight and the human interpreter agreed, that molecular weight was recorded for the peak. In some cases, all of the 20 mass spectra selected by the library search system were examined in search of those that would match the unknown spectra in all features, and a spectrum could be selected which matched particularly well and its molecular weight would be used for the peak in question. Some peaks were excluded from this treatment, including the air peak and peaks selected in error by the integration routine as part of the column bleed at the end of the chromatogram.

Analyses were performed on an Agilent GC/MS system composed of a gas chromatograph (Agilent 7890) and single quadrupole mass spectrometer (Agilent 5975N). The separations were performed using a fused silica capillary column, 30 m long with an inner diameter of 0.25mm, and coated with 0.25 μm HP-5MS nonpolar stationary phase (Agilent Catalog No. 19091S-433). Injections were made with a programmable temperature vaporization (PTV) injection port operated in constant temperature mode at 280 °C, in split mode with a split ratio of 1:200. The column operated with helium carrier gas under constant flow conditions of 1mL/min. The mass spectrometer was scanned over the range of 20-500 m/z. The ion source operated in electron impact mode (70 Volt) and the electron multiplier voltage was 1375 Volts. A 5 μL fixed needle syringe was used for injections, all of which were approximately 0.2 μL in volume. The syringe was cleaned with pentane between injections.

[1] *Wiley Registry of Mass Spectral Data*, 8th Edition, John Wiley & Sons, Hoboken, NJ, 2006.

A.3. RESULTS AND DISCUSSION

The resulting total ion chromatogram for the Exxon Mobil JP-8 sample is shown in Figure A-1. The sample integration report and peak molecular weighs are listed in Table A-1. The total ion chromatogram from the Shell SPK sample is shown in Figure A-2. The sample integration report and peak molecular weights are listed in Table A-2. The total ion chromatogram from the Camelina HRJ sample is shown in Figure A-3. The sample integration report and peak molecular weights are listed Table A-3. The total ion chromatogram from the sample of Tallow HRJ is shown in Figure A- 4. The sample integration report and peak molecular weights are listed in Table A-4. The weighted average molecular weights are summarized in Figure A-5. Note the total ion chromatograms exhibited several peaks that were common to all samples and were either determined to be air or components of the pentane syringe-wash solvent. The air peak was disregarded in the calculation of molecular weights.

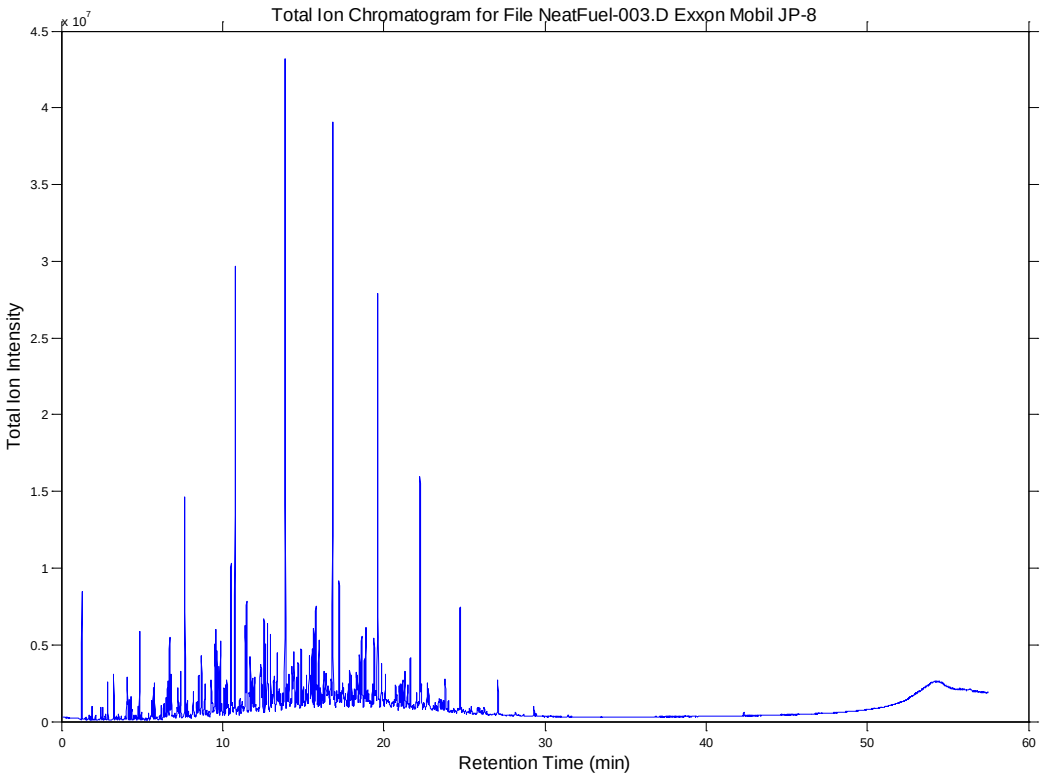

Figure A-1. Total Ion Chromatogram from Exxon Mobile JP-8

Table A-1. Peak Areas and Molecular Weights for Exxon Mobile JP-8

Sample	JP-8 Exxon-Mobile, Fairfax, VA 0.2 uL Neat-Spl				
Misc Info.	40(2.5)-300(3) @ 15, 280 °C inj, SplitFuel.M				
PK No.	RT	Area Pct	MW (Est)	MW*PctArea	Remarks
1	1.2718	0.4744	29		Air
2	1.9053	0.0532	86	4.5752	
3	2.4396	0.0542	84	4.5528	Cyclohexane and Benzene, coeluting
4	2.4617	0.0408	100	4.08	
5	2.5663	0.0701	100	7.01	
6	2.8858	0.2213	100	22.13	
7	3.2659	0.3129	98	30.6642	
8	4.0647	0.1988	114	22.6632	
9	4.1032	0.3549	92	32.6508	
10	4.2354	0.1784	114	20.3376	
11	4.3346	0.1908	112	21.3696	
12	4.3676	0.0761	112	8.5232	
13	4.7808	0.1129	112	12.6448	
14	4.8579	0.6972	114	79.4808	
15	5.6016	0.1964	128	25.1392	
16	5.7007	0.3292	112	36.8704	
17	5.7889	0.3929	126	49.5054	
18	6.1965	0.1362	126	17.1612	
19	6.3618	0.1953	128	24.9984	
20	6.494	0.2249	106	23.8394	
21	6.6152	0.6489	128	83.0592	
22	6.7198	0.9271	106	98.2726	
23	6.8135	0.5469	128	70.0032	
24	7.1936	0.1658	126	20.8908	
25	7.2432	0.3093	126	38.9718	
26	7.2982	0.1567	126	19.7442	
27	7.4084	0.5512	106	58.4272	
28	7.6673	2.0957	128	268.2496	
29	7.8105	0.1889	126	23.8014	
30	8.1961	0.3873	142	54.9966	Manual estimate
31	8.3834	0.1494	120	17.928	
32	8.4275	0.167	142	23.714	
33	8.5322	0.6172	126	77.7672	
34	8.7029	0.7595	142	107.849	
35	8.9178	0.3448	142	48.9616	

36	9.3034	0.5256	140	73.584	
37	9.3419	0.1774	142	25.1908	
38	9.5403	0.8119	120	97.428	
39	9.5843	0.8845	142	125.599	
40	9.6669	0.6587	142	93.5354	
41	9.7551	0.6126	120	73.512	
42	9.8708	0.8223	142	116.7666	
43	9.9589	0.158	140	22.12	
44	10.1021	0.3833	120	45.996	
45	10.1958	0.3296	140	46.144	
46	10.2784	0.5259	140	73.626	
47	10.35	0.1301	140	18.214	
48	10.5263	1.6997	120	203.964	
49	10.6089	0.1829	140	25.606	
50	10.7907	4.6151	142	655.3442	
51	11.0772	0.1961	134	26.2774	
52	11.2314	0.2803	156	43.7268	
53	11.4242	1.2159	120	145.908	
54	11.4958	1.2783	156	199.4148	
55	11.6666	0.3578	184	65.8352	
56	11.7272	0.6653	140	93.142	
57	11.8043	0.2393	154	36.8522	
58	11.8649	0.4956	140	69.384	
59	11.9916	0.6153	156	95.9868	
60	12.3552	0.7183	134	96.2522	
61	12.3937	0.5361	138	73.9818	
62	12.4543	0.3233	134	43.3222	
63	12.4929	0.2767	134	37.0778	
64	12.581	0.98	134	131.32	
65	12.6747	0.7566	156	118.0296	
66	12.7848	1.4573	156	227.3388	
67	12.9832	0.9145	156	142.662	
68	13.0768	0.2756	154	42.4424	
69	13.1484	0.3613	134	48.4142	
70	13.198	0.5632	134	75.4688	
71	13.3963	1.0851	134	145.4034	
72	13.4624	0.2806	154	43.2124	
73	13.523	0.2839	154	43.7206	
74	13.5891	0.2335	154	35.959	
75	13.7378	0.426	154	65.604	
76	13.8921	7.1826	156	1120.486	

77	13.9857	0.6935	148	102.638	
78	14.1179	0.5569	152	84.6488	
79	14.2556	0.258	170	43.86	
80	14.3272	0.6918	148	102.3864	
81	14.4429	1.2411	134	166.3074	
82	14.6027	0.5948	152	90.4096	
83	14.7018	0.7427	170	126.259	
84	14.8836	0.8771	154	135.0734	
85	14.9773	0.2013	148	29.7924	
86	15.0103	0.3029	168	50.8872	
87	15.1701	0.2518	148	37.2664	
88	15.2142	0.4416	148	65.3568	
89	15.3023	0.2951	168	49.5768	
90	15.3904	1.1491	134	153.9794	
91	15.5116	0.5023	170	85.391	
92	15.5557	0.8672	170	147.424	
93	15.6603	0.9317	170	158.389	
94	15.787	1.3728	172	236.1216	
95	15.8476	0.3005	148	44.474	
96	15.9799	0.7832	170	133.144	
97	16.0735	0.3751	148	55.5148	
98	16.1837	0.3559	166	59.0794	
99	16.2883	0.5471	128	70.0288	
100	16.4261	0.7246	168	121.7328	
101	16.4866	0.1372	170	23.324	
102	16.5362	0.3705	168	62.244	
103	16.7456	0.7262	166	120.5492	
104	16.8447	6.4386	170	1094.562	
105	16.9549	0.2692	162	43.6104	
106	17.0926	0.3198	162	51.8076	
107	17.1532	0.2601	162	42.1362	
108	17.2413	1.5094	184	277.7296	
109	17.346	0.2906	182	52.8892	
110	17.4562	0.5312	182	96.6784	
111	17.5113	0.3401	166	56.4566	
112	17.6159	0.3778	162	61.2036	
113	17.8032	0.3307	182	60.1874	
114	17.9023	0.5171	168	86.8728	
115	18.007	0.5224	182	95.0768	
116	18.0952	0.1555	162	25.191	
117	18.2053	0.3562	182	64.8284	

118	18.321	0.4996	184	91.9264	
119	18.3761	0.3964	184	72.9376	
120	18.5028	0.857	184	157.688	
121	18.635	1.1729	184	215.8136	
122	18.8113	0.587	184	108.008	
123	18.8884	0.9344	198	185.0112	
124	18.9931	0.325	196	63.7	
125	19.0592	0.1733	196	33.9668	
126	19.3126	0.3068	182	55.8376	
127	19.4117	1.0231	142	145.2802	
128	19.5109	0.3041	196	59.6036	
129	19.6321	4.6968	184	864.2112	
130	19.8689	0.5971	142	84.7882	
131	19.9351	0.1651	198	32.6898	
132	20.1113	0.4683	198	92.7234	
133	20.6787	0.127	196	24.892	
134	20.7448	0.3226	182	58.7132	
135	20.8164	0.1824	196	35.7504	
136	20.9762	0.3318	198	65.6964	
137	21.0533	0.4004	198	79.2792	
138	21.18	0.4463	198	88.3674	
139	21.3122	0.5896	198	116.7408	
140	21.4885	0.5015	198	99.297	
141	21.6537	0.7071	212	149.9052	
142	22.0449	0.3355	196	65.758	Mixture of unidentified saturated hydrocarboon and ethyl naphthalene isomer
143	22.2597	2.7509	198	544.6782	
144	22.3423	0.5314	156	82.8984	dimethyl naphthalene isomer
145	22.7059	0.412	156	64.272	
146	22.7885	0.459	156	71.604	
147	23.422	0.1575	196	30.87	
148	23.4716	0.243	196	47.628	
149	23.5818	0.1978	212	41.9336	
150	23.714	0.1424	212	30.1888	
151	23.8186	0.5806	226	131.2156	
152	24.017	0.1473	212	31.2276	
153	24.7386	1.1111	212	235.5532	
154	27.0908	0.4215	226	95.259	
155	29.3218	0.1047	240	25.128	
156	53.6865	0.266			Artifact

157	54.05	0.2696			Artifact
158	54.2263	0.2003			Artifact
	Totals	98.7893		15570.81	
Weighted Average MW:				157.6164	

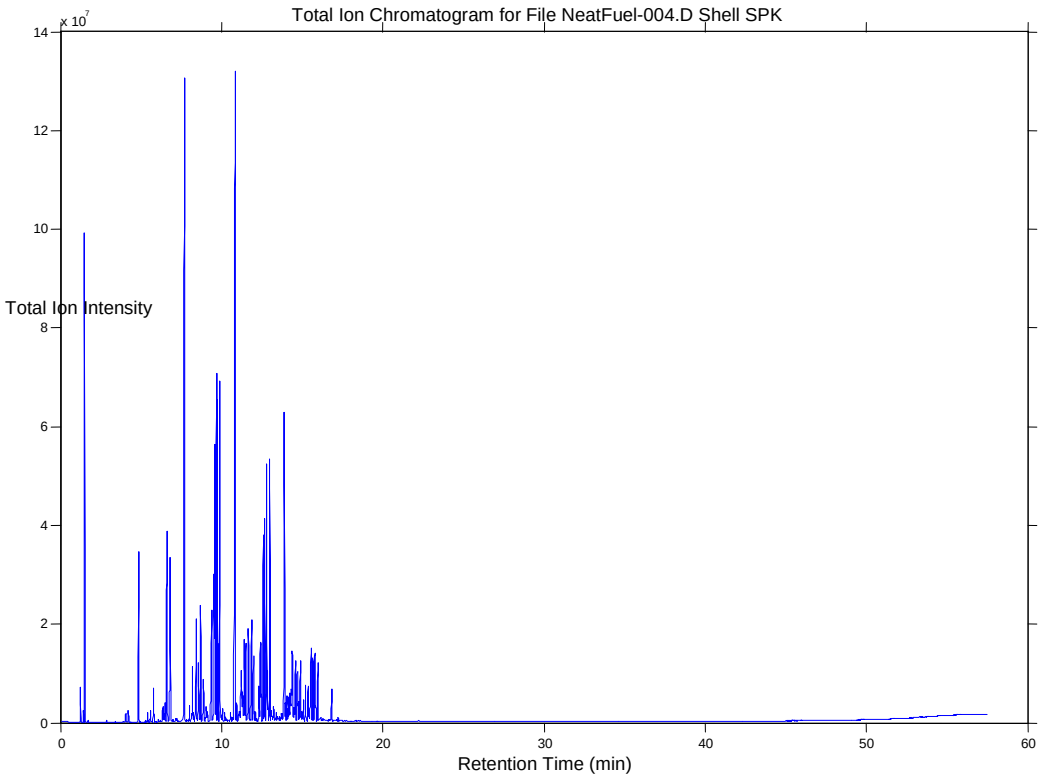

Figure A-2. Total Ion Chromatogram from Shell SPK

Table A-2. Peak Areas and Molecular Weights for Shell SPK-8

Sample	Shell SPK 0.2 uL Neat-Spl SplitFuel-8Apr11-3				
Misc Info.	40(2.5)-300(3)@15, 280 °C inj				
PK	RT	Area Pct	MW Est.	MW*PctArea	Remarks
1	1.2609	0.1338	29		Air peak
2	1.4537	0.0434	72	3.1248	Part of the solvent?
3	1.5088	3.3591	72	241.8552	Part of the solvent?
4	1.5419	0.4966	72	35.7552	Part of the solvent?
5	4.0538	0.0629	114	7.1706	
6	4.0869	0.0352	114	4.0128	
7	4.2246	0.1078	114	12.2892	
8	4.8526	1.4165	114	161.481	
9	5.42	0.0904	128	11.5712	
10	5.5907	0.1258	128	16.1024	
11	5.7725	0.3853	128	49.3184	
12	6.0865	0.0328	128	4.1984	
13	6.3564	0.1633	128	20.9024	
14	6.428	0.1151	128	14.7328	
15	6.4941	0.1918	128	24.5504	
16	6.6208	2.8228	128	361.3184	
17	6.8136	2.084	128	266.752	
18	7.1882	0.0286	128	3.6608	
19	7.2378	0.0265	126	3.339	
20	7.7115	13.5645	128	1736.256	
21	8.0145	0.1753	142	24.8926	
22	8.1302	0.0854	142	12.1268	
23	8.2018	0.5939	142	84.3338	
24	8.2679	0.0904	128	11.5712	
25	8.3726	0.2327	142	33.0434	
26	8.4277	1.1019	142	156.4698	
27	8.5654	0.8913	142	126.5646	
28	8.7031	1.2302	142	174.6884	
29	8.8794	0.8123	142	115.3466	
30	9.0006	0.0476	142	6.7592	
31	9.0612	0.2028	142	28.7976	
32	9.1273	0.1148	142	16.3016	
33	9.3862	1.8325	142	260.215	
34	9.5404	1.656	142	235.152	

35	9.5955	3.3497	142	475.6574	
36	9.6891	4.2237	142	599.7654	
37	9.7773	0.7508	142	106.6136	
38	9.893	4.3431	142	616.7202	
39	9.9646	0.0677	156	10.5612	
40	10.0582	0.1875	142	26.625	
41	10.2014	0.1122	140	15.708	
42	10.565	0.1272	142	18.0624	
43	10.6972	0.0559	156	8.7204	
44	10.857	16.3314	142	2319.059	
45	10.9451	0.1941	156	30.2796	
46	11.0828	0.1174	156	18.3144	
47	11.1379	0.1158	156	18.0648	
48	11.2371	0.9916	156	154.6896	
49	11.2977	0.3447	156	53.7732	
50	11.3417	0.2627	156	40.9812	
51	11.4189	1.0314	156	160.8984	
52	11.5015	0.8115	156	126.594	
53	11.6668	1.5359	156	239.6004	
54	11.8155	0.2242	156	34.9752	
55	11.8706	1.1275	156	175.89	
56	11.9918	0.9652	156	150.5712	
57	12.1019	0.1018	156	15.8808	
58	12.1735	0.0384	154	5.9136	
59	12.3168	0.3693	156	57.6108	
60	12.4049	0.9943	156	155.1108	
61	12.4545	0.2801	156	43.6956	
62	12.5867	2.0578	156	321.0168	
63	12.6859	2.116	156	330.096	
64	12.8015	2.8622	156	446.5032	
65	12.8621	0.5065	156	79.014	
66	12.9943	2.8238	156	440.5128	
67	13.0825	0.1302	170	22.134	
68	13.1265	0.0564	170	9.588	
69	13.2257	0.2819	170	47.923	
70	13.3965	0.1265	170	21.505	
71	13.4681	0.0582	154	8.9628	
72	13.5121	0.0578	154	8.9012	
73	13.6168	0.0747	170	12.699	
74	13.7049	0.0884	170	15.028	
75	13.738	0.0996	170	16.932	

76	13.8978	4.1665	156	649.974	
77	13.9639	0.2116	170	35.972	
78	14.052	0.272	170	46.24	
79	14.1236	0.146	170	24.82	
80	14.1952	0.3059	170	52.003	
81	14.2613	0.3333	170	56.661	
82	14.3329	0.4819	170	81.923	
83	14.388	1.3903	170	236.351	
84	14.4982	0.1429	170	24.293	
85	14.5918	0.8947	170	152.099	
86	14.7075	0.6833	170	116.161	
87	14.7736	0.2626	170	44.642	
88	14.9003	0.8602	170	146.234	
89	14.9664	0.1092	170	18.564	
90	15.0876	0.2965	170	50.405	
91	15.2143	0.3887	170	66.079	
92	15.3686	0.4296	170	73.032	
93	15.5118	0.4132	170	70.244	
94	15.5503	0.8204	170	139.468	
95	15.6605	0.6953	170	118.201	
96	15.7872	0.7573	170	128.741	
97	15.8368	0.1615	170	27.455	
98	15.98	0.6178	170	105.026	
99	16.8339	0.3606	170	61.302	
100	17.236	0.0502	184	9.2368	
	Total Pcnt	99.8661		14260.93	
Weighted Average MW:			142.8005		
Note, this treatment excluded the air peak at the beginning of the run.					

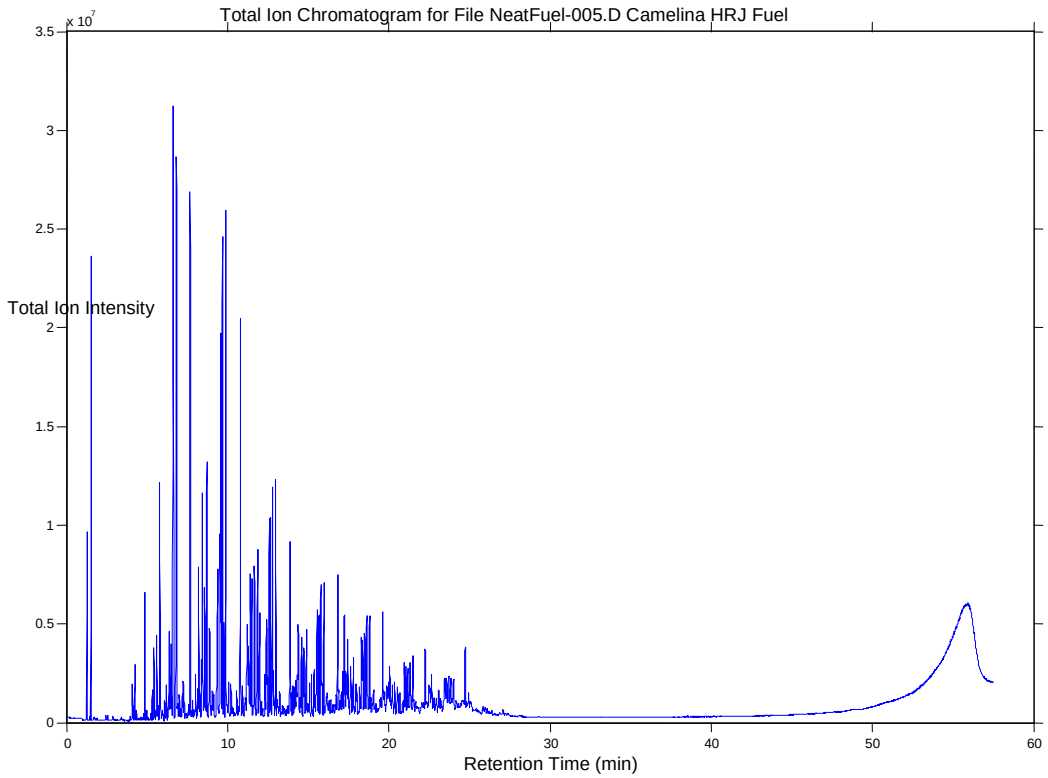

Figure A-3. Total Ion Chromatogram from Camelina HRJ

Table A-3. Peak Areas and Molecular Weights for Camelina HRJ

Sample	Camelina HRJ 0.2 uL high split				
Misc Info.	40(2.5)-300(3)@15, 280 °C inj				
PK	RT	Area Pct	MW Est.	MW*PctA	Remarks
1	1.2773	0.3431	29		Air
2	1.5252	0.7296	72	52.5312	Pentane solvent
3	4.0812	0.1392	114	15.8688	
4	4.1142	0.0548	114	6.2472	
5	4.2464	0.2419	114	27.5766	
6	4.3456	0.0217	112	2.4304	
7	4.8744	0.518	114	59.052	
8	4.9846	0.0428	112	4.7936	
9	5.3316	0.1244	128	15.9232	
10	5.4418	0.309	128	39.552	
11	5.5024	0.0589	128	7.5392	
12	5.6126	0.4825	128	61.76	
13	5.7172	0.0674	112	7.5488	
14	5.7943	1.1381	128	145.6768	
15	5.8384	0.2183	128	27.9424	
16	6.1083	0.1212	128	15.5136	
17	6.213	0.1886	126	23.7636	
18	6.3783	0.4593	128	58.7904	
19	6.4499	0.3026	128	38.7328	
20	6.5105	0.3585	128	45.888	
21	6.6372	4.5413	128	581.2864	
22	6.83	3.32	128	424.96	
23	6.9126	0.1271	126	16.0146	
24	7.0062	0.1314	126	16.5564	
25	7.0834	0.0795	126	10.017	
26	7.2046	0.1737	128	22.2336	
27	7.2542	0.2005	126	25.263	
28	7.3147	0.0936	126	11.7936	
29	7.5792	0.1001	128	12.8128	
30	7.6783	2.4688	128	316.0064	
31	7.8326	0.1081	126	13.6206	
32	7.9207	0.0677	126	8.5302	
33	8.0253	0.2648	142	37.6016	
34	8.141	0.1612	142	22.8904	
35	8.2127	0.841	142	119.422	
36	8.2788	0.187	142	26.554	

37	8.3889	0.2831	142	40.2002	
38	8.444	1.1973	142	170.0166	
39	8.5762	1.0299	142	146.2458	
40	8.7195	1.4147	142	200.8874	
41	8.8902	0.9431	142	133.9202	
42	9.0169	0.0838	140	11.732	
43	9.072	0.2035	142	28.897	
44	9.1381	0.1645	142	23.359	
45	9.3584	0.5848	142	83.0416	
46	9.3915	0.8436	142	119.7912	
47	9.5457	0.9936	142	141.0912	
48	9.5953	1.8785	142	266.747	
49	9.6835	2.3208	142	329.5536	
50	9.7771	0.478	142	67.876	
51	9.8873	2.5054	142	355.7668	
52	9.9534	0.1313	156	20.4828	
53	10.0691	0.2724	156	42.4944	
54	10.2123	0.2209	140	30.926	
55	10.2839	0.0817	140	11.438	
56	10.5759	0.2008	156	31.3248	
57	10.7026	0.0878	156	13.6968	
58	10.7962	2.079	142	295.218	
59	10.9339	0.2313	156	36.0828	
60	11.0882	0.1248	156	19.4688	
61	11.1377	0.1178	156	18.3768	
62	11.2149	0.4679	156	72.9924	
63	11.2369	0.4466	156	69.6696	
64	11.303	0.437	142	62.054	
65	11.3471	0.2412	156	37.6272	
66	11.4187	0.8956	156	139.7136	
67	11.5068	0.6973	156	108.7788	
68	11.6005	0.0659	156	10.2804	
69	11.6666	1.2375	156	193.05	
70	11.8153	0.215	156	33.54	
71	11.8704	0.9616	156	150.0096	
72	11.9971	0.7691	156	119.9796	
73	12.1073	0.0904	156	14.1024	
74	12.3221	0.2215	156	34.554	
75	12.4102	0.6218	156	97.0008	
76	12.4543	0.2112	156	32.9472	
77	12.5865	1.0403	156	162.2868	

78	12.6801	1.0187	156	158.9172	
79	12.7958	1.1952	156	186.4512	
80	12.8619	0.2703	156	42.1668	
81	12.9886	1.237	156	192.972	
82	13.0878	0.1161	170	19.737	
83	13.2365	0.2501	170	42.517	
84	13.3963	0.1007	170	17.119	
85	13.4734	0.0575	154	8.855	
86	13.7433	0.1348	170	22.916	
87	13.8866	1.0661	156	166.3116	
88	13.9637	0.1277	170	21.709	
89	14.0518	0.1612	170	27.404	
90	14.1289	0.1016	170	17.272	
91	14.195	0.1961	170	33.337	
92	14.2611	0.2046	170	34.782	
93	14.3383	0.2913	170	49.521	
94	14.3878	0.8907	170	151.419	
95	14.498	0.0976	170	16.592	
96	14.5917	0.5701	170	96.917	
97	14.7073	0.4515	170	76.755	
98	14.7679	0.1438	170	24.446	
99	14.9001	0.5998	170	101.966	
100	14.9718	0.0699	170	11.883	
101	15.0929	0.2345	170	39.865	
102	15.2196	0.2155	170	36.635	
103	15.3739	0.2886	170	49.062	
104	15.5557	0.9285	170	157.845	
105	15.6658	0.5822	170	98.974	
106	15.7925	0.7358	170	125.086	
107	15.8421	0.1939	170	32.963	
108	15.9798	0.6887	170	117.079	
109	16.1506	0.2179	184	40.0936	
110	16.1892	0.132	184	24.288	
111	16.3048	0.1055	184	19.412	
112	16.3985	0.1408	184	25.9072	
113	16.5472	0.0991	184	18.2344	
114	16.6849	0.0622	184	11.4448	
115	16.7455	0.1686	184	31.0224	
116	16.8392	0.774	170	131.58	
117	16.8943	0.1188	184	21.8592	
118	16.9604	0.0845	184	15.548	

119	17.0705	0.2548	184	46.8832	
120	17.1532	0.3104	184	57.1136	
121	17.2413	0.7627	184	140.3368	
122	17.357	0.2855	184	52.532	
123	17.4066	0.1308	184	24.0672	
124	17.4672	0.42	184	77.28	
125	17.5223	0.1036	184	19.0624	
126	17.6489	0.4223	184	77.7032	
127	17.8032	0.3931	184	72.3304	
128	17.9685	0.1841	184	33.8744	
129	18.018	0.1406	184	25.8704	
130	18.1998	0.1764	184	32.4576	
131	18.321	0.449	184	82.616	
132	18.3761	0.397	184	73.048	
133	18.5028	0.4996	184	91.9264	
134	18.635	0.6514	184	119.8576	
135	18.8168	0.5475	184	100.74	
136	18.8829	0.0758	198	15.0084	
137	18.9655	0.037	198	7.326	
138	19.0096	0.0492	198	9.7416	
139	19.0647	0.1179	198	23.3442	
140	19.4668	0.1058	198	20.9484	
141	19.5274	0.1038	198	20.5524	
142	19.6266	0.6425	184	118.22	
143	19.7367	0.184	198	36.432	
144	19.891	0.2099	198	41.5602	
145	20.0011	0.3738	198	74.0124	
146	20.0672	0.4455	198	88.209	
147	20.2325	0.2324	198	46.0152	
148	20.3702	0.2369	198	46.9062	
149	20.53	0.1791	198	35.4618	
150	20.585	0.1183	198	23.4234	
151	20.6897	0.1488	198	29.4624	
152	20.8825	0.0792	198	15.6816	
153	20.9762	0.3539	198	70.0722	
154	21.0533	0.3113	198	61.6374	
155	21.18	0.3324	198	65.8152	
156	21.3122	0.4441	198	87.9318	
157	21.494	0.4325	198	85.635	
158	21.6647	0.097	184	17.848	
159	22.0559	0.184	198	36.432	

160	22.166	0.0705	198	13.959	
161	22.2597	0.452	198	89.496	
162	22.4965	0.2326	212	49.3112	
163	22.5681	0.2363	198	46.7874	
164	22.6618	0.3083	212	65.3596	
165	22.7444	0.0635	198	12.573	
166	22.8161	0.1194	212	25.3128	
167	22.9648	0.1296	226	29.2896	
168	23.1025	0.2037	212	43.1844	
169	23.2182	0.0824	212	17.4688	
170	23.422	0.0868	226	19.6168	
171	23.5046	0.3744	212	79.3728	
172	23.5818	0.2887	212	61.2044	
173	23.7195	0.2891	212	61.2892	
174	23.8462	0.2765	212	58.618	
175	24.0224	0.342	212	72.504	
176	24.1877	0.1302	226	29.4252	
177	24.7441	0.3637	212	77.1044	
178	24.9534	0.1081	212	22.9172	
179	54.0004	3.1422			Column Bleed Artifacts
180	55.9064	20.0647			Column Bleed Artifacts
181	57.0963	0.0104			Column Bleed Artifacts
	Total:	76.4401		11898.95	
Weighted Average MW:		155.6637			
Note, this treatment excluded the air peak at the beginning of the run.					

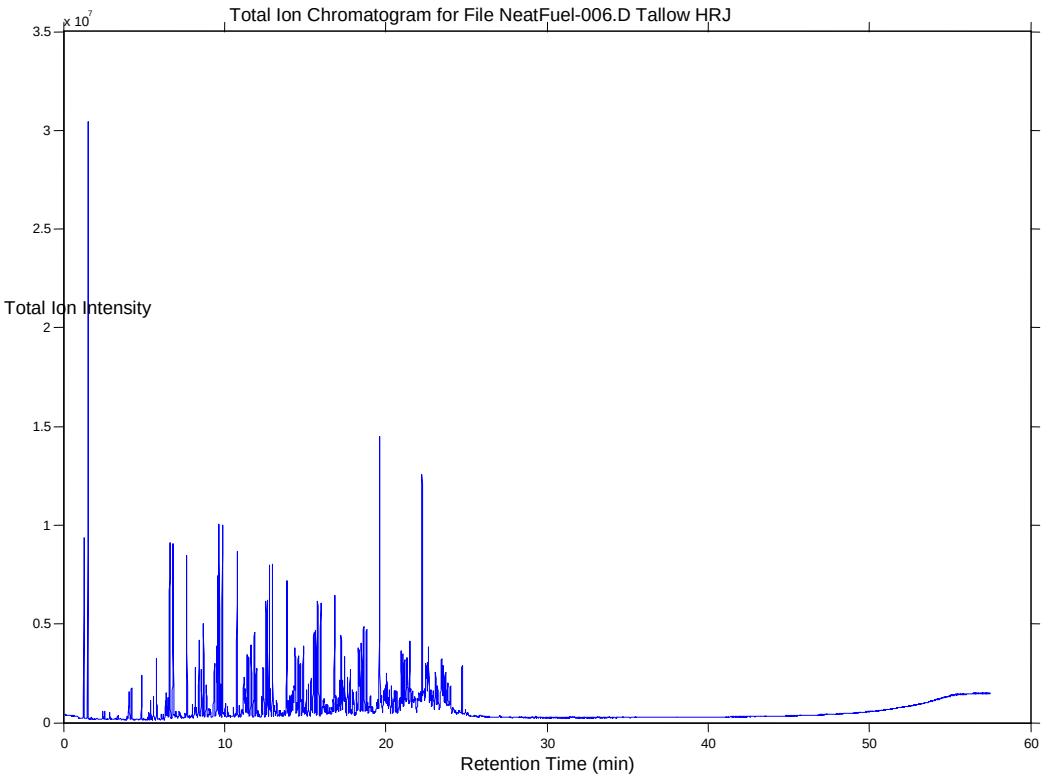

Figure A- 4. Total Ion Chromatogram from Tallow HRJ

Table A-4. Peak Areas and Molecular Weights from Tallow HRJ

Sample	Tallow HRJ 0.2 uL high split				
Misc Info.	40(2.5)-300(3) @ 15, 280 °C inj				
PK	RT	Area Pct	MW Est	MW*PctA	Remarks
1	1.2776	0.7025	29	20.3725	Air
2	1.5255	2.3238	72	167.3136	Solvent Pentane
3	4.0705	0.225	114	25.65	
4	4.098	0.0648	114	7.3872	
5	4.2357	0.3074	114	35.0436	
6	4.8637	0.3942	114	44.9388	
7	5.4256	0.1648	128	21.0944	
8	5.6019	0.272	128	34.816	
9	5.7837	0.753	128	96.384	
10	6.3621	0.3117	128	39.8976	
11	6.4337	0.1945	128	24.896	
12	6.4998	0.2157	128	27.6096	
13	6.6155	2.7832	128	356.2496	
14	6.8138	1.9256	128	246.4768	
15	7.6621	1.6177	128	207.0656	
16	8.0147	0.1676	142	23.7992	
17	8.1304	0.1107	142	15.7194	
18	8.1965	0.5847	142	83.0274	
19	8.2681	0.1048	127	13.3096	
20	8.3727	0.1877	142	26.6534	
21	8.4278	0.893	142	126.806	
22	8.5655	0.7581	128	97.0368	
23	8.7033	1.0679	142	151.6418	
24	8.874	0.634	142	90.028	
25	9.3477	0.4402	142	62.5084	
26	9.3808	0.5765	142	81.863	
27	9.5295	0.7479	142	106.2018	
28	9.5791	1.4912	142	211.7504	
29	9.6672	1.9923	142	282.9066	
30	9.7664	0.3528	142	50.0976	
31	9.8711	2.0331	142	288.7002	
32	10.0529	0.1988	142	28.2296	
33	10.2016	0.126	142	17.892	
34	10.5652	0.1093	156	17.0508	
35	10.7855	1.8182	142	258.1844	
36	10.9232	0.1551	156	24.1956	

37	11.2262	0.8195	156	127.842	
38	11.2923	0.3829	156	59.7324	
39	11.3364	0.2116	156	33.0096	
40	11.408	0.8295	156	129.402	
41	11.4961	0.6739	156	105.1284	
42	11.6559	1.2555	156	195.858	
43	11.8101	0.1803	156	28.1268	
44	11.8597	1.0004	156	156.0624	
45	11.9864	0.7577	156	118.2012	
46	12.3114	0.2284	156	35.6304	
47	12.3995	0.6677	156	104.1612	
48	12.4436	0.237	156	36.972	
49	12.5758	1.259	156	196.404	
50	12.6695	1.2718	156	198.4008	
51	12.7852	1.6679	156	260.1924	
52	12.8513	0.3314	156	51.6984	
53	12.978	1.6954	156	264.4824	
54	13.0771	0.1537	170	26.129	
55	13.2314	0.3397	170	57.749	
56	13.8814	1.7009	156	265.3404	
57	13.953	0.186	170	31.62	
58	14.0466	0.2403	170	40.851	
59	14.1237	0.1358	170	23.086	
60	14.1899	0.2988	170	50.796	
61	14.256	0.3266	170	55.522	
62	14.3276	0.4601	170	78.217	
63	14.3827	1.4271	170	242.607	
64	14.4928	0.155	184	28.52	
65	14.5865	0.9314	184	171.3776	
66	14.7022	0.7669	170	130.373	
67	14.7628	0.2219	170	37.723	
68	14.895	0.9908	170	168.436	
69	15.0823	0.3856	170	65.552	
70	15.2144	0.3645	170	61.965	
71	15.3687	0.5038	170	85.646	
72	15.545	1.6091	170	273.547	
73	15.6607	1.0244	170	174.148	
74	15.7874	1.3483	170	229.211	
75	15.8314	0.3275	170	55.675	
76	15.9747	1.2578	170	213.826	
77	16.0958	0.1135	184	20.884	

78	16.1454	0.1934	184	35.5856	
79	16.184	0.2062	184	37.9408	
80	16.3878	0.226	184	41.584	
81	16.7403	0.2773	184	51.0232	
82	16.834	1.4766	170	251.022	
83	16.8891	0.1954	184	35.9536	
84	17.0653	0.433	184	79.672	
85	17.148	0.5323	184	97.9432	
86	17.2361	1.3108	184	241.1872	
87	17.3518	0.5001	184	92.0184	
88	17.4014	0.233	184	42.872	
89	17.462	0.7177	184	132.0568	
90	17.6438	0.7317	184	134.6328	
91	17.798	0.6723	156	104.8788	
92	17.9633	0.3267	184	60.1128	
93	18.0128	0.2483	184	45.6872	
94	18.1946	0.3432	184	63.1488	
95	18.3213	0.8345	184	153.548	
96	18.3709	0.7659	184	140.9256	
97	18.4976	0.9086	184	167.1824	
98	18.6298	1.286	184	236.624	
99	18.8116	1.0951	184	201.4984	
100	18.8832	0.1689	198	33.4422	
101	19.0595	0.2838	198	56.1924	
102	19.4616	0.2176	170	36.992	
103	19.5222	0.2429	170	41.293	
104	19.6269	3.4807	184	640.4488	
105	19.7315	0.3151	198	62.3898	
106	19.8858	0.4307	198	85.2786	
107	19.996	0.7519	198	148.8762	
108	20.0676	0.8632	198	170.9136	
109	20.1557	0.1913	198	37.8774	
110	20.2273	0.4464	198	88.3872	
111	20.365	0.4754	198	94.1292	
112	20.5303	0.331	198	65.538	
113	20.5854	0.3085	170	52.445	
114	20.6845	0.3563	198	70.5474	
115	20.8773	0.2302	168	38.6736	
116	20.9765	0.963	198	190.674	
117	21.0536	0.8763	198	173.5074	
118	21.1803	0.8965	198	177.507	

119	21.3125	1.0845	198	214.731	
120	21.4888	0.9478	198	187.6644	
121	21.5439	0.4605	212	97.626	
122	21.6595	0.3827	212	81.1324	
123	22.0066	0.2869	212	60.8228	
124	22.0562	0.3342	212	70.8504	
125	22.1058	0.3033	212	64.2996	
126	22.1664	0.3202	184	58.9168	
127	22.26	3.1566	198	625.0068	
128	22.3481	0.3655	212	77.486	
129	22.3922	0.3647	212	77.3164	
130	22.4969	0.967	212	205.004	
131	22.574	1.0706	212	226.9672	
132	22.6621	1.2764	212	270.5968	
133	22.7392	0.2965	226	67.009	
134	22.8109	0.4726	212	100.1912	
135	22.9155	0.2887	198	57.1626	
136	22.9651	0.3455	198	68.409	
137	23.1028	0.9406	212	199.4072	
138	23.2185	0.4312	226	97.4512	
139	23.4223	0.3823	226	86.3998	
140	23.4719	0.6678	212	141.5736	
141	23.505	0.6469	212	137.1428	
142	23.5821	0.8433	212	178.7796	
143	23.7198	0.8238	212	174.6456	
144	23.8465	0.5894	226	133.2044	
145	24.0173	0.486	212	103.032	
146	24.7389	0.5754	212	121.9848	
	Total:	99.2974		16779.55	
Weighted Average MW:		168.9828			
Note, this treatment excluded the air peak at the beginning of the run.					

Figure A-5. Molecular Weight Summary

Sample	Weighted Average MW (g/mol)
JP-8	158
Camelina HRJ	156
Tallow HRJ	169
Shell SPK	143

Appendix B: Flame Detector Data

Table B-1 lists the data collected on how many counts/s were recorded by Det-Tronics UV and IR sensors from a 1 ft × 1 ft pan fire at a 100 ft distance.

Table B-1. UV and IR Detector Counts

FUEL	Counts / s	
	UV	IR
JP-8	37	44
Camelina	42	61
Camelina 50/50	40	62
Tallow	41	55
Tallow 50/50	36	49
Shell	40	47
Shell 50/50	42	53

B-1.2.

LIST OF SYMBOLS, ABBREVIATIONS, AND ACRONYMS

Å	ångstrøm = 10^{-10} meters
AFRL	Air Force Research Laboratory
ASC/WNN	Aeronautical Systems Center Alternative Fuels Certification Division
°C	Celsius
CGD	combustible gas detectors
eV	electron volt
ETL	Engineering Technical Letter
FID	Flame Ionization Detector
FM	Factory Mutual
°F	Fahrenheit
F-T	Fischer-Tropsch
g/mol	grams per mole
GC/MS	gas chromatography/mass spectrometry
HEFA	hydroprocessed esters and fatty acids
HRJ	hydroprocessed renewable jet
IR	infrared
JP-8	Jet Propellant 8
LEL	lower explosive limit
MSA	Mine Safety Appliances
MSDS	Material Safety Data Sheet
MW	molecular weight
m/z	mass-to-charge ratio (of an ion)
NFPA	National Fire Protection Association
OFDs	optical flame detectors
PID	photoionization detector
s	second(s)
SE&V	support equipment and vehicles
SPK	synthetic paraffinic kerosene
TIC	total ion chromatogram
TLV	threshold limit value
TO	Technical Order
UV	ultraviolet
USAF	United States Air Force